TOWARDS DEVELOPING A WATERSHED ASSESSMENT FRAMEWORK USING GEOMORPHIC-BASED HYDROLOGIC AND HYDRAULIC MODELING

A Thesis Presented for the

Master of Science

Degree

The University of Tennessee, Knoxville

Matthew J. Tolson

August 2024

Copyright © 2024 by Matthew J. Tolson
All rights reserved.

ACKNOWLEDGEMENTS

I would like to thank my primary advisor, Dr. Schwartz, for all of his guidance, expertise, and patience shown throughout my time as a graduate student. I would also like to thank my committee members, Dr. Hathaway and Dr. He, for their support and excellent classes. Furthermore, I would like to thank Mrs. Parks Oliver for her continual support and comradery. Dr. Simpson and Mr. Song also deserve thanks for their guidance and frequent progress meeting attendance.

Additionally, I would like to thank my partner, Claudia, and my mother, Shelly, for their overwhelming support. From continually reviewing work to enduring my ramblings, I appreciate their love tremendously.

Lastly, I would like to thank the Tennessee Water Resources Research Center (TNWRRC) for supporting my research and the Town of Farragut for providing spatial data for this study.

ABSTRACT

Urban hydromodification has created a need for an urban watershed assessment framework involving environmental rehabilitation practices to prioritize long-term and cost-effective enhancement strategies. This study sought to develop a watershed-scale model using Personal Computer Storm Water Management Model (PCSWMM) and field reconnaissance to be included in the planning phase of future watershed assessment frameworks. Typical modeling efforts for urban watershed stormwater management plans do not consider fluvial geomorphology during model development. To create an effective stormwater management and stream restoration watershed plan, this study sought to determine the level of model development necessary to prioritize watershed enhancement activities and explore the correlation among stream field data, desktop data, and modeled stream power and bed shear stress. A case study was completed on the Turkey Creek watershed in Knox County, Tennessee. Within the study scope, the effectiveness of geomorphic node placement and inclusion of stormwater control measures (SCMs) into models were assessed. A watershed assessment plan was developed including rapid geomorphic assessments (RGAs), a hydraulic grade control (HGC) inventory, geomorphic-based analysis where reaches were determined, three watershed-scale models with increasing detail, and stream power and bed shear stress metrics calculated from model outputs. $\Omega_{30,50,80}$ [percentile stream power] and $\tau_{30,50,80}$ [percentile bed shear stress] were calculated from model outputs and statistically analyzed. The three models were: (I) PCSWMM automated conveyance network, (II) developed conveyance network of geomorphic-based nodes and links, and (III) Model II with SCMs. The most detailed model, Model III, outperformed other simulations indicating that watershed models should incorporate geomorphic node placement, SCMs, desktop data, field verification, and manual adjustment of automatically generated features. Single and stepwise linear multiple regression analyses yielded varying results, but field (RGA score and sub-metrics) and desktop (drainage area, channel slope, land uses, distance between HGCs) data were determined to be predictors of $\Omega_{30,50,80}$ and $\tau_{30,50,80}$. RGA sub-metrics, land use data, and distance to HGCs were frequently included in exclusive multiple regressions, suggesting that field and desktop data should be incorporated during model development. Building a geomorphic-based watershed

planning model provides stormwater managers key information to locate areas of instability and test rehabilitation techniques.

TABLE OF CONTENTS

CHAPTER ONE INTRODUCTION 1
Background 1
Urban Hydromodification and the Importance of Effective Impervious Area (EIA) 1
Overview of Stormwater Control Measures (SCMs) 2
Overview of Stream Restoration 3
Effectiveness of Stormwater Control Measures (SCMs) versus Stream Restoration in Urban Watersheds 4
Stormwater Management Planning: Current Issues and Potential Solutions 6
Environmental Protection Agency (EPA) Storm Water Management Model (SWMM) 9
Stream Power as a Watershed-Scale Stream Assessment Tool 10
Rapid Geomorphic Assessment (RGA) and the Importance of Hydraulic Grade Controls (HGCs) 11
Knowledge Gaps and Objectives 12
CHAPTER TWO METHODS 14
Site Selection 14
Rapid Geomorphic Assessment (RGA) and Watershed Reach Determination/Designation 14
Installation and Location of Stage Recorder and Discharge Measurements 16
Watershed-Scale Model Development 16
Model I 19
Model II 21
Model III 23
Geomorphic/Model Analysis 28
Stream Power and Bed Shear Stress Determination for Model Reaches 28
Percentile Stream Power and Bed Shear Stress Determination for Analysis Reaches 28
Single Regression Analysis 29
Stepwise Linear Multiple Regression Analysis 29
CHAPTER THREE RESULTS 31
Watershed Reach Determination/Designation 31

Rapid Geomorphic Assessment (RGA) Scores 31
Model Reach Maximum Stream Power and Bed Shear Stress Maps 31
Single Regression Analysis Results 40
Stepwise Linear Multiple Regression Analysis Results 40
CHAPTER FOUR DISCUSSION 63
Suggested Level of Model Development for Watershed Management Planning 63
Correlation Among Field Reconnaissance Data, Desktop-Gathered Data, and Percentile Stream Power and Bed Shear Stress 65
Benefits of Geomorphic-Based Modeling Approach for Urban Watershed Planning 65
Conclusions and Recommendations 67
LIST OF REFERENCES 69
VITA 74

LIST OF TABLES

Table 1: RGA Scores 32
Table 2: Percentile Bed Shear Stress and Stream Power per Analysis Reach 41
Table 3: Single Regression Analysis Results 48
Table 4: 30th-Percentile Bed Shear Stress Exclusive Stepwise Linear Multiple Regression Analysis Results 49
Table 5: 50th-Percentile Bed Shear Stress Exclusive Stepwise Linear Multiple Regression Analysis Results 50
Table 6: 80th-Percentile Bed Shear Stress Exclusive Stepwise Linear Multiple Regression Analysis Results 51
Table 7: 30th-Percentile Stream Power Exclusive Stepwise Linear Multiple Regression Analysis Results 52
Table 8: 50th-Percentile Stream Power Exclusive Stepwise Linear Multiple Regression Analysis Results 53
Table 9: 80th-Percentile Stream Power Exclusive Stepwise Linear Multiple Regression Analysis Results 54
Table 10: 30th-Percentile Bed Shear Stress Inclusive Stepwise Linear Multiple Regression Analysis Results 55
Table 11: 50th-Percentile Bed Shear Stress Inclusive Stepwise Linear Multiple Regression Analysis Results 56
Table 12: 80th-Percentile Bed Shear Stress Inclusive Stepwise Linear Multiple Regression Analysis Results 57
Table 13: 30th-Percentile Stream Power Inclusive Stepwise Linear Multiple Regression Analysis Results 58
Table 14: 50th-Percentile Stream Power Inclusive Stepwise Linear Multiple Regression Analysis Results 59
Table 15: 80th-Percentile Stream Power Inclusive Stepwise Linear Multiple Regression Analysis Results 60

LIST OF FIGURES

Figure 1: Study Drainage Area with RGAs and Analysis Reaches 15
Figure 2: TNWRRC Monitoring Gauge Observed Water Depths 17
Figure 3: Stage-Discharge Relationship 18
Figure 4: Model I 20
Figure 5: Magnified View of Model I 20
Figure 6: Model II 22
Figure 7: Magnified View of Model II 22
Figure 8: Red Mill Dam 24
Figure 9: Model III 25
Figure 10: Magnified View of Model III 25
Figure 11: Example Outlet Structure in Turkey Creek Watershed 27
Figure 12: Example RGA 33
Figure 13: Model I Maximum Bed Shear Stress Map 34
Figure 14: Model II Maximum Bed Shear Stress Map 35
Figure 15: Model III Maximum Bed Shear Stress Map 36
Figure 16: Model I Maximum Stream Power Map 37
Figure 17: Model II Maximum Stream Power Map 38
Figure 18: Model III Maximum Stream Power Map 39
Figure 19: Model I Relationship Between RGA Score and Percentile Bed Shear Stress 42
Figure 20: Model II Relationship Between RGA Score and Percentile Bed Shear Stress 43
Figure 21: Model III Relationship Between RGA Score and Percentile Bed Shear Stress 44
Figure 22: Model I Relationship Between RGA Score and Percentile Stream Power 45
Figure 23: Model II Relationship Between RGA Score and Percentile Stream Power 46
Figure 24: Model III Relationship Between RGA Score and Percentile Stream Power 47

LIST OF ATTACHMENTS

A: ArcGIS Pro Layers..... ArcGISProLayers.zip
B: Maximum Bed Shear Stress and Stream Power Calculations.....MaxShearandSPCalcs.zip
C: Model Files .....ModelFiles.zip
D: Multiple Regression Files .....MultipleRegressionFiles.zip
E: RGA Forms and Protocols .....RGAFormsandProtocols.zip
F: Single Regression Files .....SingleRegressionFiles.zip
G: Stage Discharge Data.....StageDischargeData.zip

CHAPTER ONE
INTRODUCTION

Background

Urban Hydromodification and the Importance of Effective Impervious Area (EIA)

Urban hydromodification occurs when new development increases watershed imperviousness leading to significant changes in hydrology and degradation of receiving streams (Hawley, Russell, & Taniguchi-Quan, 2022; Walsh et al., 2005). Stream degradation yields negative impacts such as infrastructure destruction, habitat alteration, increased water treatment costs, diminished reservoir capacities, and decreased biodiversity (Woockman & Schwartz, 2018). Because the side effects of urban hydromodification can be costly, existing studies have explored the drivers and outcomes of stream degradation in urban watersheds.

The urban stream syndrome, a concept coined by Walsh et al., (2005), describes the observed ecological degradation of streams that drain urban land. Hydrologically, the infiltration and transpiration capacities in an urban watershed decrease, resulting in increased runoff volume, flashier hydrographs, increased stream high flow rates, and decreased stream baseflow. In turn, urban streams undergo cycles of geomorphic instability and degrade systematically (Hawley, Russell, & Taniguchi-Quan, 2022). Hydromodification alters sediment transport capacity and supply, which drives streams to become sediment supply limited if channel erosive resistance properties are insufficient (Woockman & Schwartz, 2018). Riparian buffers can provide erosive resistance and filtration of nutrients or other pollutants, but urban streams often have inadequate buffers to offset the effects of hydromodification. Furthermore, the riparian buffers' influence on stream condition decreases as the area of the catchment directly connected to streams by stormwater pipes increases (Vietz et al., 2014; Walsh et al., 2005). Without hydraulic grade controls (HGCs) preventing vertical downcutting of the channel and/or lateral migration, a domino effect can occur as streams lose structural stability, nutrient removal capability, biological function, and infiltration capacity (Woockman & Schwartz, 2018). The domino effect that is the urban stream syndrome is primarily driven by conventional stormwater infrastructure impacts (Hawley, Russell, & Taniguchi-Quan, 2022). Even with the use of traditional stormwater control

measures (SCMs) to mitigate increases in effective impervious area, streams undergo hydrologic and geomorphic change (Epps & Hathaway, 2018; Vietz et al., 2014).

Effective Impervious Area (EIA) is defined as the impervious area hydrologically connected to streams by piped drainage networks or other stormwater infrastructure (Epps & Hathaway, 2018). Compared to total impervious area (TIA), EIA more accurately represents urban hydrology as EIA produces a greater proportion of storm-event runoff and flashier hydrographs. Vietz et al., (2014) conducted a study to determine if EIA is a better predictor than TIA of geomorphic impairment in streams. The study showed that EIA is more accurate than TIA (EIA coefficient of determination (R^2) ≥ 0.44 and TIA $R^2 \geq 0.22$) and that measurable geomorphic changes occur even at low levels of EIA (0-3%). Based on field-collected discharge and rainfall data for a forested watershed with low EIA (Burns et al., 2012), Vietz et al., (2014) also showed that EIA and discharge are directly proportional (2% increase in EIA yields almost 2% increase in discharge), which highlights the effect of urbanization on stream stability. EIA has the potential to provide stormwater managers the ability to assess structurally or ecologically vulnerable areas within a watershed, since EIA is an indicator of excessive stream erosion and is proportional to stream biological condition (Walsh et al., 2005). However, measuring EIA is often difficult since stormwater pipe inventories are often incomplete or mischaracterized due to the challenge in measuring and verifying underground infrastructure (Epps & Hathaway, 2018). To better estimate EIA for stormwater planning, a spatial model may be calibrated and refined utilizing a high-resolution digital elevation model (DEM), accurate rainfall data, and observational data. Once EIA is determined, managers can alter the model to reflect SCM installation. A living watershed-scale spatial model has the potential to simulate the effects of urban hydromodification and improvement by SCM implementation or stream restoration.

Overview of Stormwater Control Measures (SCMs)

Urban stormwater management has gradually shifted focus from simply draining cities towards maintaining a balance between meeting human needs and preserving geomorphic and ecological watershed functions (Burns et al., 2012; Rodak et al., 2020). In the United States, the Federal Water

Pollution Control Act of 1948, which became the Clean Water Act in 1972, enacted quality standards for surface waters (Wu, Wu, & Zhang, 2019). In the 1990s, the United States identified stormwater runoff as an agent of environmental damage to coastal bay areas which led to new stormwater management objectives globally (Burns et al., 2012). Over the next several decades, SCMs were developed and became tools used by stormwater managers to attenuate quantity and improve quality of surface runoff (Rodak et al., 2020). Types of SCMs include erosion and sediment control, constructed stormwater ponds, constructed stormwater wetlands, bioretention, permeable pavement, green roofs, and rainwater harvesting. SCMs offer an alternative to conventional stormwater management, but research suggests their performance is not adequate to mitigate urban hydromodification (Burns et al., 2012; Walsh et al., 2015). An issue is that land developed without SCMs (prior to the 1990s) is heavily impacted by urban hydromodification. Any municipality is a mix of land development with and without SCMs causing various degrees of stream channel degradation and the need for stream restoration (McCleary, 1999). Additionally, increased duration of storm flows, reduction of base flows, and potential for treatment SCMs to misfunction often lead to habitat and ecological degradation (Burns et al., 2012). Consequently, the need for innovation is evident as the number of urban stormwater publications released per year has rapidly increased over the past decade (Wu, Wu, & Zhang, 2019). Improving the design and placement of SCMs is a significant topic of urban stormwater research especially concerning the cumulative effectiveness of SCMs at a watershed-scale (Rodak et al., 2020).

Overview of Stream Restoration

Following the adoption of the Clean Water Act, the Wetland Restoration Act of 1990 set conservation practices for wetlands in 1990 and was the first law to mention the restoration of degraded stream ecosystems as a mitigation practice (dos Reis Oliveira et al., 2020). In 2008, stream restoration was solidified as compensatory mitigation under the Clean Water Act Section 404. Stream restoration practices often aim to rehabilitate a degraded ecosystem to an approximation of its remaining natural potential by returning streams to a state of dynamic equilibrium (Shields et al., 2003). Typical strategies include vertically controlling grade by installing hard points in the channel bed, laterally controlling grade using hard bank armoring or

soil bioengineering, reconnecting a channel to its floodplain or constructing a channel forming discharge (bankfull) bench to relieve shear during high flow events, installing in-stream structures to direct flow and provide habitat, reestablishing a riparian buffer, and providing a pool-riffle sequence to promote dynamic sediment transport and habitat. Most stream restoration projects involve channel realignment or reconstruction based on regional curves for hydraulic geometry and reference reaches (dos Reis Oliveira et al., 2020; Shields et al., 2003). Despite the stream restoration industry growing rapidly since 2008, monitoring and long-term evaluation of projects remain lacking (Rubin, Kondolf, & Rios-Touma, 2017). Common metrics of project success include aerial measurements like acreage and stream length restored which are not adequate to evaluate complex ecosystems (Rubin, Kondolf, & Rios-Touma, 2017). These metrics inadvertently influence the types of projects undertaken by practitioners, since more profit is generated from projects with large restorable area and stream length. Additionally, stream restoration techniques primarily aim toward morphological improvements under the assumption that ecological uplift and water quality improvement will occur over time (dos Reis Oliveira et al., 2020; Rubin, Kondolf, & Rios-Touma, 2017). To ensure success, site-specific ecological objectives must be set at the start of a project rather than relying on assumptions. In urban settings, projects may not be successful if sources of runoff and pollution are not addressed (Bernhardt & Palmer, 2011; Walsh, Fletcher, & Ladson, 2005). However, urban projects can be successful without focusing on ecological uplift by limiting chronic channel erosion (Hawley, Russell, & Taniguchi-Quan, 2022). Limiting channel erosion protects existing vegetation, habitat, and infrastructure which is a primary concern in urban settings. Ultimately, setting clear objectives is key to a successful stream restoration project (Rubin, Kondolf, & Rios-Touma, 2017; Walsh et al., 2016).

Effectiveness of Stormwater Control Measures (SCMs) versus Stream Restoration in Urban Watersheds

SCM implementation to mitigate runoff and pollutant sources in urban watersheds has been researched over the past few decades due to raised awareness of the effects of hydromodification (Anim et al., 2019; Earles et al., 2020; Murphy et al., 2022; Walsh et al., 2015; Walsh, Fletcher,

& Ladson, 2005). Compared to stream restoration, which is a localized effort, SCMs potentially offer a more effective strategy to improve watershed ecology and water quality (Anim et al., 2019). For the purpose of this study, research performed in both the United States and Australia are presented to illustrate the ongoing discussion of SCM and stream restoration effectiveness. These countries are the top two producers of urban stormwater publications from 1980-2019 with more than 50% of the total number of publications released (Wu, Wu, & Zhang, 2019). The Australian research effort focused on ecological uplift from watershed-scale SCM implementation (Anim et al., 2019; Walsh et al., 2015; Walsh, Fletcher, & Ladson, 2005), whereas the United States effort consisted of case-studies exploring the success of stream restoration projects with and without SCM implementation (Earles et al., 2020; Murphy et al., 2022). Ultimately, there is growing understanding that stream restoration efforts in combination with SCMs may be the best method of mitigating the effects of urban hydromodification (Woockman & Schwartz, 2018). Existing case studies are described below.

The Australian research effort largely focused on SCMs and discounted stream restoration as the sole answer to combating urban hydromodification. Walsh, Fletcher, & Ladson, (2005) modeled redesigned drainage networks for 15 watersheds near Melbourne, Australia, and found that ecological uplift in streams can be generated from implementing EIA-reducing design measures throughout a catchment. Anim et al., (2019) modeled SCM scenarios for the McMahons Creek watershed near Melbourne and found that a 65% reduction in runoff volume is required to reestablish pre-development hydrologic conditions and protect the hydraulic environment. Little Stringybark Creek, which was a modeled watershed in Walsh, Fletcher, & Ladson, (2005), became a watershed-scale experiment that involved implementing 289 stormwater retention systems with the goal of increasing in-stream ecology. This community research effort surfaced issues with large-scale SCM implementation such as finding space for SCMs, finding demand for harvested stormwater, and measuring short-term ecological success (Walsh et al., 2015), which were also problems highlighted in Anim et al., (2019). At the time of publishing, no ecological improvement had been observed from SCM implementation by Walsh et al., (2015) likely due to the need for more SCMs to address watershed impacts (Walsh et al., 2016; Walsh, Fletcher, & Ladson, 2005).

Multiple case-studies in the United States outline the effectiveness of SCMs and stream restoration, ultimately, promoting stream restoration or a joint SCM and stream restoration effort to generate uplift in urban watersheds. Earles et al., (2020) relied solely on stream restoration to successfully reduce pollutant loads at Cherry Creek in Denver, Colorado. The alternative strategy to stream restoration was implementing extended dry detention basins (EDBs), which are a type of SCM. The pollutant load reduction potential of stream restoration was determined to be equivalent to more than 100 regional EDBs or nearly 1,000 subregional EDBs (Earles et al., 2020). Another stream restoration project in Colorado, South Platte, was partially successful since floodplain processes and aquatic habitat improved, but runoff and pollutant sources were not assessed (Murphy et al., 2022). The South Platte project highlights the need to assess runoff sources since vegetation was unable to establish, resulting in secondary channel siltation. A project in Maryland, Little Seneca Creek, jointly used stream restoration with SCMs to protect water quality and sensitive biota. Despite mitigating peak flows and runoff volumes, water quality degraded and target species were lost (Murphy et al., 2022). These case-studies raise the need for further research into ecological uplift in urban watersheds partly through redesigning SCMs with an ecological focus (Walsh et al., 2016). In theory, SCMs and stream restoration as a combined practice provide urban streams necessary structural uplift and the potential to generate ecological uplift. Although this combination of practices has great potential to combat urban hydromodification, issues surrounding watershed planning and policy largely prevent implementation (Woockman & Schwartz, 2018).

Stormwater Management Planning: Current Issues and Potential Solutions

As understanding of hydraulic and hydrologic principles associated with watershed health has grown over the past several decades, the need for improved policy and practice surrounding stormwater management planning has become increasingly evident among researchers (Bernhardt & Palmer, 2011; Earles et al., 2020; Hawley, Russell, & Taniguchi-Quan, 2022; Prosser, Morison, & Coleman, 2015; Walsh et al., 2016; Woockman & Schwartz, 2018). Current policy and practice follow traditional techniques that focus on human needs like water provision and flood mitigation, whereas research promotes techniques that focus on water quality improvement and ecosystem

health which inherently provide human needs (Walsh et al., 2015; Woockman & Schwartz, 2018). To experience the potential benefits of a healthy watershed including an improved water supply, flood mitigation, terrestrial biodiversity, urban cooling, resilience to climate change, urban agriculture, and human well-being, institutional change must occur involving researchers, policy makers, developers, and the public (Walsh et al., 2016).

The current issues with stormwater management planning are largely associated with policy lag time, poor design standards, and new development (Bernhardt & Palmer, 2011; Earles et al., 2020; Prosser, Morison, & Coleman, 2015; Walsh et al., 2016; Walsh et al., 2015; Woockman & Schwartz, 2018). These problems are driven by politics as well as the need for cost-effective and easy-to-use restoration/rehabilitation solutions resulting in ongoing segregation of science and practice. In fact, changes to watershed restoration policies often lag a decade or more behind science and research allowing practitioners to design projects based on outdated information (Bernhardt & Palmer, 2011). Even when restoration practices involving streams or SCMs are implemented, positive impacts may not be achieved because of existing issues with design standards. Traditionally, regulatory efforts have used uniform SCM standards that serve as umbrella solutions that lack consideration for channel protection. Although peak storm flows are reduced, durations of high flow are often increased by SCMs inducing more work-performing flow on channel erosive elements (Woockman & Schwartz, 2018). Similarly, stream restoration projects may not improve a watershed because work performed is sometimes limited to being “in kind” which rules out riparian enhancement and the elimination of watershed impacts (Bernhardt & Palmer, 2011). A further issue is that ecological uplift is often mitigated indirectly as a product of structural improvements, meaning that watershed health likely remains poor (Bernhardt & Palmer, 2011; Walsh, Fletcher, & Ladson, 2005). Watershed health can be undermined by new development even after stream restoration and SCM implementation takes place (Prosser, Morison, & Coleman, 2015; Walsh et al., 2016; Walsh et al., 2015). New development acts as a watershed impact, and the issue is that the development process in most areas is a competition for money and space and often involves political influence. At any point during a restoration project, new development within the watershed has the potential to cause the project to fail (Prosser, Morison, & Coleman, 2015; Walsh et al., 2016; Walsh et al., 2015). To successfully implement

restoration/rehabilitation projects within a watershed, institutional change must occur to focus on a holistic watershed management approach while emphasizing human benefits to stakeholders and fostering trustful relationships among researchers, managers, decision-makers, and the public (Earles et al., 2020; Prosser, Morison, & Coleman, 2015; Walsh et al., 2015).

Researchers largely agree that watershed management should operate using an interdisciplinary and holistic approach and, thus, have proposed principles addressing the current issues surrounding stormwater management planning and restoration practices (Earles et al., 2020; Hawley, Russell, & Taniguchi-Quan, 2022; Prosser, Morison, & Coleman, 2015; Walsh et al., 2016). In this context, a holistic watershed management approach seeks to address impacts rather than simply treating symptoms, and an interdisciplinary approach aims to improve ecological health and water quality by involving ecologists, hydrologist, geomorphologists, and engineers in restoration projects (Earles et al., 2020; Walsh et al., 2016). With these approaches in practice, regulatory agencies can require evidence beyond structural enhancement such as improved water quality, ecological abundance or diversity, or restored environmental flows to better predict and monitor watershed health (Bernhardt & Palmer, 2011; Earles et al., 2020). When monitoring these parameters, restoring environmental flows to a predevelopment state is a prerequisite to achieving necessary flow and water-quality regimes for successful stream restoration (Anim et al., 2019; Vietz et al., 2014; Walsh et al., 2016). Beyond restoration and rehabilitation, developers must be controlled by governance to prevent new catchment impacts from undermining watershed improvements which requires agreement across multiple agencies (Prosser, Morison, & Coleman, 2015; Walsh et al., 2015). This agreement poses a challenge to stormwater managers because they typically do not hold much political and financial power compared to developers (Walsh et al., 2016). To overcome these issues, the human benefits of holistic watershed management need to be emphasized to decision-makers, and relationships among various involved parties must be built on trust (Earles et al., 2020; Prosser, Morison, & Coleman, 2015; Walsh et al., 2015). Once these relationships are founded, innovation can be achieved by clearly articulating the value of healthy stream ecosystems and the management actions that will be required (Walsh et al., 2016). Despite the potential for innovation, stormwater managers continue to have limited funding and need a way to prioritize projects.

Stormwater management governance is often subject to social and institutional resistance making innovation difficult due to limited funding or regulatory incentives (Cousins & Hill, 2021; Rieck et al., 2022; Walsh et al., 2016; Zhao, Fonseca, & Zeerak, 2019). Therefore, a need exists for stormwater managers to develop a watershed assessment framework involving SCM implementation, conservation, and stream restoration to determine long-term and cost-effective watershed enhancement strategies (Hawley, Russell, & Taniguchi-Quan, 2022; Woockman & Schwartz, 2018). Within this framework, mitigation efforts can be prioritized through master planning, design, and construction (Earles et al., 2020). This strategy of planning, designing, and constructing is successful but time consuming and costly. A more cost-effective way to plan and prioritize restoration projects is to build a model that tests the effectiveness of SCM implementation and stream restoration within a watershed (Woockman & Schwartz, 2018). Using a model to perform stormwater management planning could allow managers to better allocate funding and enhance watersheds without having to overcome institutional obstacles that may take decades to overcome.

Environmental Protection Agency (EPA) Storm Water Management Model (SWMM)

The EPA SWMM model is suitable for urban watershed assessment and management, since the model can simulate sewer and stormwater networks, open channels, backwater effects, subcatchments consisting of pervious and impervious areas, and low impact developments (LIDs) (Niazi et al., 2017). SWMM is a dynamic rainfall-runoff simulation model capable of utilizing design storm precipitation or continuous, historical rainfall data (Rossman, 2017; Rossman & Huber, 2015; Rossman & Simon, 2022). Traditionally, SWMM has been used for flood analysis (Niazi et al., 2017; Rossman & Simon, 2022), but recent focus has shifted to climate change impacts (Niazi et al., 2017). The runoff component of SWMM consists of rain gauges, subcatchments, aquifers, snow packs, unit hydrographs, and LIDs, whereas the routing component consists of nodes, outfalls, dividers, storage units, conduits, pumps, orifices, weirs, and outlets (Rossman, 2017; Rossman & Huber, 2015; Rossman & Simon, 2022; Woockman & Schwartz, 2018). SWMM is not typically used to model process-level details, as most models are created to assess broad areas like watersheds (Niazi et al., 2017). SWMM is capable of modeling urban

hydromodification within a watershed since subcatchments default to draining runoff from impervious areas directly to pipes or channels unless otherwise specified by the user (Rossman & Huber, 2015). Commercial versions of SWMM are available such as Personal Computer Storm Water Management Model (PCSWMM) that offer automated and more effective methods of calibration (Niazi et al., 2017). Sensitive parameters for calibrating SWMM models include conduit geometry, impervious percentage, impervious depression storage, and Manning's roughness coefficient for conduits and impervious area. SWMM has the potential to facilitate watershed assessment and planning by identifying vulnerable areas within a watershed and allowing managers to test improvements prior to construction.

Stream Power as a Watershed-Scale Stream Assessment Tool

Stream power relates to channel morphology and stability and can be used as a central parameter for analysis when assessing streams at a watershed scale (Bizzi & Lerner, 2015; Lea & Legleiter, 2016; Vocal Ferencevic & Ashmore, 2012). Total stream power is the energy expenditure per unit distance along a channel. Incorporating variable channel width, specific stream power is the energy expenditure per unit area along a channel and indicates channel stability as high stream power produces geomorphic responses in streams (Bizzi & Lerner, 2015; Hawley, Russell, & Taniguchi-Quan, 2022). Stream power is a function of discharge and energy slope, which have been determined using various methods in literature. In three studies, a DEM was used to estimate energy slope. Vocal Ferencevic & Ashmore, (2012) determined DEM slope estimates to be statistically similar to HEC-RAS modeled water surface slope (water surface slope approximates energy slope). Discharge was estimated by a discharge to drainage area relationship (Lea & Legleiter, 2016), a calibrated runoff model (Vocal Ferencevic & Ashmore, 2012), and empirical relationships (Bizzi & Lerner, 2015). Bizzi & Lerner, 2015 recommend modeling hydrology for discharge rather than relying on empirical relationships. From mapping stream power of Soda Butte Creek in Yellowstone National Park (Lea & Legleiter, 2016) and the Highland Creek Watershed in Ontario, Canada (Vocal Ferencevic & Ashmore, 2012), slope was determined to have a greater effect on stream power than discharge, and stream power was found to not vary linearly downstream. The rapid changes in slope and stream power in the Highland Creek

Watershed were attributed to the presence of barriers and engineered structures throughout the watershed. With watershed information such as substrate data, channel geometries, and an HGC inventory, specific stream power can be used to identify locations of excessive channel erosion. Stream power as a watershed-scale stream assessment tool can be achieved by coupling SWMM modeling with process-based field reconnaissance.

Rapid Geomorphic Assessment (RGA) and the Importance of Hydraulic Grade Controls (HGCs)

Channel adjustment and instability from hydromodification causes downcutting and lateral erosion (channel incision) (Simon & Darby, 1999; Simon & Downs, 1995). An assessment procedure was developed to estimate the potential for channel incision to occur and/or continue. RGAs present an efficient method for stormwater managers to assess streams throughout a watershed using a process-based approach. Traditionally, a one-size-fits-all approach to management schemes have ignored factors like substrate data, HGCs, channel planform, and proximity to geomorphic thresholds (Bledsoe et al., 2012). A process-based approach like an RGA should incorporate these factors in addition to a channel evolution model (CEM) (Bledsoe et al., 2012; Booth & Fischenich, 2015). A well-known CEM is the representation of a stream undergoing incision due to watershed urbanization (Booth & Fischenich, 2015) and is included in the Natural Resources Conservation Science (NRCS) Stream Restoration Design Handbook as a six-stage process (Li, 2008). Building an HGC inventory while performing RGAs is integral to process-based stream assessment since HGCs provide bed stability and significantly affect sediment transport (Hawley, Russell, & Taniguchi-Quan, 2022). Examples of natural HGCs include beaver dams, large woody debris jams, and bedrock outcrops, while artificial examples include weirs, bridges, culverts, sills, and armored beds (Woockman & Schwartz, 2018). Depending on the level of sediment transport influence, HGCs can trigger local responses taking the form of channel widening, upstream aggradation, and/or downstream incision (Booth & Fischenich, 2015; Woockman & Schwartz, 2018). In urban watersheds, the potential for bed stability is increased due to the prevalence of artificial HGCs, but the potential for lateral stability is decreased by riparian vegetation disturbances (Woockman &

Schwartz, 2018). RGAs incorporating HGCs and a CEM are necessary to successfully build a watershed-scale stream assessment model using stream power as the central parameter.

Knowledge Gaps and Objectives

Based on existing studies, there is a need for an urban watershed assessment framework involving environmental rehabilitation practices to determine and prioritize long-term and cost-effective enhancement strategies (Hawley, Russell, & Taniguchi-Quan, 2022; Woockman & Schwartz, 2018). Earles et al., (2020) recommend that restoration efforts under an assessment framework be prioritized through master planning, design, and construction, but this approach may be time consuming and costly. Therefore, this study sought to develop a watershed-scale model using PCSWMM and basic field reconnaissance to be included in the planning and prioritization phase of future watershed assessment frameworks. Typical SWMM modeling efforts for urban watershed stormwater management plans do not consider fluvial geomorphology during model development. To create an effective stormwater management watershed plan and provide geomorphic-based reaches (model links) for a stream restoration plan, SWMM node placement must be based on geomorphic criteria. This study utilized RGAs to assess streams using a process-based approach while building an HGC inventory for model node placement. The level of model development necessary to plan and prioritize watershed enhancement activities is unexplored as studies typically aim to build models with as much detail as is available. Additionally, the correlation among field reconnaissance data, desktop-gathered data, and geomorphic-based modeled stream power and bed shear stress remains untested in existing studies.

The objectives of this study were to determine the level of model development necessary to plan and prioritize watershed enhancement activities, SCM implementation and/or stream restoration, and to explore the correlation among field reconnaissance data, desktop-gathered data, and modeled stream power and bed shear stress for a portion of the Turkey Creek watershed in Knox County, Tennessee. Within the scope of the study, the respective effectiveness of geomorphic node placement and inclusion of SCMs into watershed-scale models were assessed. RGAs were performed, an HGC inventory was compiled, geomorphic-based analysis reaches were determined, three watershed-scale models were developed, stream power and bed shear stress metrics were

calculated and visualized from model outputs, and percentile stream power and bed shear stress metrics were calculated from model outputs and statistically analyzed to accomplish the study objectives.

CHAPTER TWO
METHODS

Site Selection

An approximately 2,958 hectare portion of the Turkey Creek watershed in Knox County, Tennessee including Turkey Creek and North Fork Turkey Creek was selected for study due to data availability and the high level of urbanization in the watershed (87.2% developed space according to the 2021 National Land Cover Database (NLCD)). Selecting a highly urbanized watershed offered ample opportunity to identify hydraulic grade controls (HGCs) and perform diverse rapid geomorphic assessments (RGAs). In terms of modeling feasibility, a monitoring gauge maintained by the Tennessee Water Resources Research Center (TNWRRC) located downstream of the historic Red Mill Dam yielded calibration data for modeling purposes. Additionally, stormwater infrastructure spatial data was provided by the Town of Farragut.

Rapid Geomorphic Assessment (RGA) and Watershed Reach Determination/Designation

Eighteen RGAs were performed along the mainstems of Turkey Creek and North Fork Turkey Creek at locations between major HGCs (Figure 1). The RGA protocol used was a modified version of the Channel Stability Index (CSI) that excludes rankings for streams influenced by bridges (Simon & Downs, 1995) (Attachment E). Individual ranking score categories included primary bed material, bed/bank protection, degree of incision, degree of constriction, stream bank erosion, stream bank instability, established riparian woody-vegetative cover, occurrence of bank accretion, and stage of channel evolution. A total score of 11 or less suggested channel stability, a score greater than 11 and less than 19 suggested moderate stability, and a score greater than 19 suggested channel instability (Simon & Klimetz, 2008). Additionally, an HGC inventory was compiled and coupled with the RGA data to designate a total of 19 geomorphic-based reaches for analysis (Figure 1). Analysis reaches were determined/designated by assigning RGA scores to spatially corresponding stream segments split by major HGCs, changes in land use, or major stream confluences, since RGAs represented unique segments of main channel in terms of geomorphology and land use.



Figure 1: Study Drainage Area with RGAs and Analysis Reaches

Installation and Location of Stage Recorder and Discharge Measurements

For model calibration purposes, a stage recorder gauge maintained by the TNWRRC was installed downstream of the Red Mill Dam, and discharge measurements were collected per United States Geological Survey (USGS) methodology (Buchanan & Somers, 1969). The gauge was installed downstream of the dam to prevent the need for individual gauges on North Fork Turkey Creek and Turkey Creek. Observed depth measurements were available from March 17th, 2022, at 5:00 P.M. to September 14th, 2023, at 8:30 A.M (Figure 2). A total of 5 discharge measurements were periodically gathered to create a stage-discharge relationship (Figure 3). Observed depths and discharge measurements were included in Attachment G.

Watershed-Scale Model Development

Three watershed-scale rainfall/runoff-routing coupled models (Models I, II, and III) were developed with increasing levels of drainage network and infrastructure detail using PCSWMM. The purpose of building three models was to assess the effectiveness of incorporating geomorphic-based node placement and SCMs as well as to showcase the level of model development necessary to provide enough information to prioritize projects from a stormwater management perspective. Desktop data and PCSWMM tools were used to build all three models, while geomorphic-based node selection and field verification were only utilized in Models II and III. SCMs were included in Model III as the only distinction from Model II. All models used the Soil Conservation Science (SCS) Curve Number (CN) infiltration method and the dynamic wave routing method. Models ran for over 10 years from October 1st, 2012, at 1:00 A.M. to September 30th, 2023, at 11:00 P.M. with time steps for runoff and routing equal to 1 hour and 5 minutes, respectively. Maximum and minimum daily temperature readings from the National Oceanic and Atmospheric Administration (NOAA) McGhee Tyson Airport monitoring station in Alcoa, Tennessee (NOAA Identification USW00013891) were included in the model and used to automatically compute evaporation. Although default snow melt and areal depletion values were used, snow effects were not analyzed. Additionally, wind speed was not considered in the models as monthly averages were set to 0 kilometers per hour. Hourly rainfall data was included from the USGS Beaver Creek monitoring station near Powell, Tennessee (USGS Identification 03535200) and set as the rain gauge for all

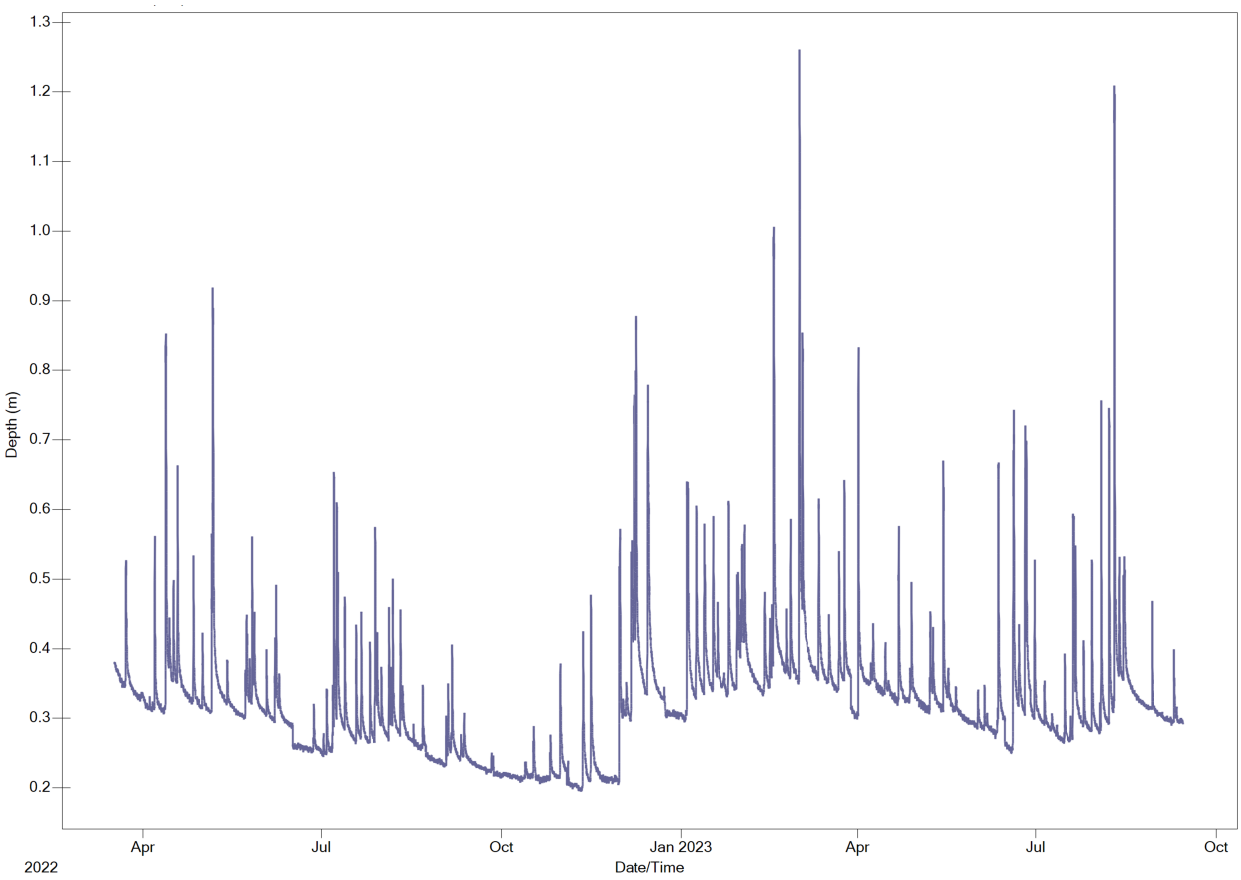


Figure 2: TNWRRC Monitoring Gauge Observed Water Depths

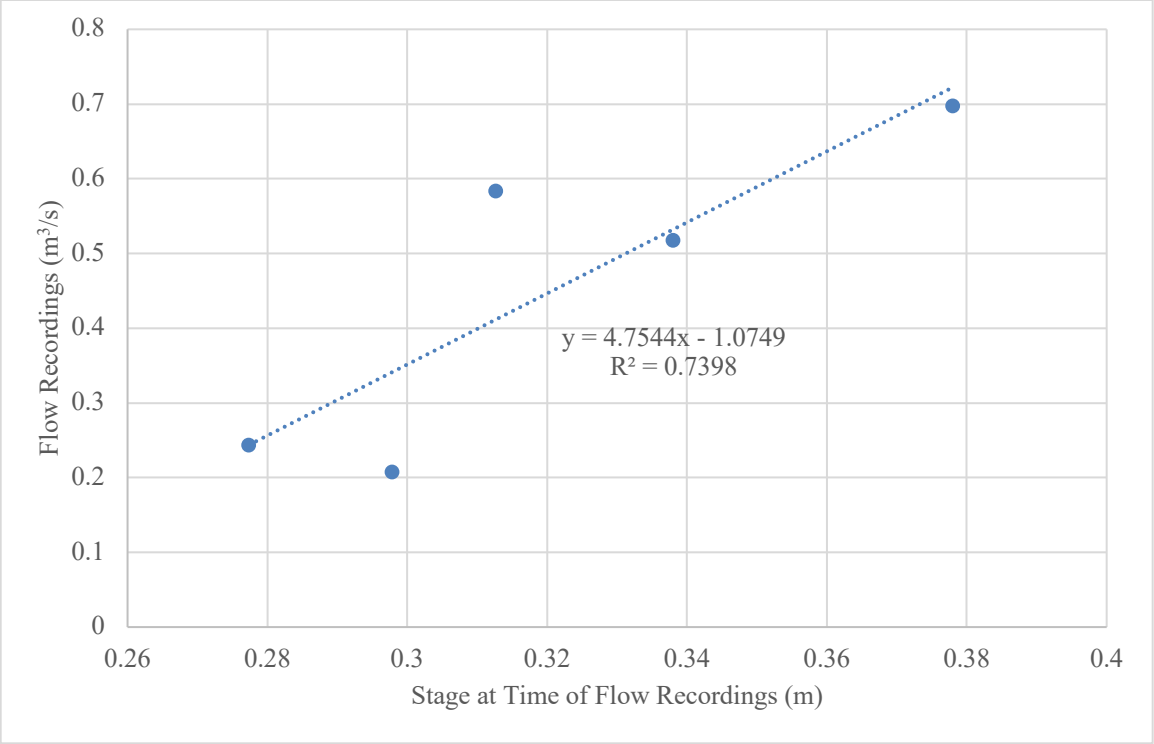


Figure 3: Stage-Discharge Relationship

subcatchments in all three models. The coordinate system used in PCSWMM and ArcGIS Pro was NAD 1983 UTM Zone 16N. Descriptions of each model's purpose and unique development process were included in the following sections.

Model I

Model I was built using desktop data and automated PCSWMM tools to serve as a low-developed model (Figures 4 and 5). The conveyance network consisting of nodes, conduits, and subcatchments was built automatically using the Watershed Delineation Tool (WDT). WDT input parameters included a USGS 1 meter digital elevation model (DEM) from 2016, an outfall located just downstream of the TNWRRC monitoring gauge (the downstream extent of the model), and a target discretization level of 20 hectares. The elevations from DEM tool was used to set the elevation of the outfall before running the WDT. The WDT automatically processed the DEM, created a drainage network from the DEM, and placed nodes at channel confluences and subcatchment outlets. The elevations from DEM tool was used again to assign node elevations, and the Transect Creator tool was used to generate irregular open channel geometries from the DEM. Cross-section lines (transect lines) were automatically drawn spatially and then over the DEM with a spacing of 30.5 meters and a length of 200 meters. When multiple transect lines intersected a given conduit, the Transect Creator tool was set to average transect lines before assigning channel geometries (transect objects) to conduits. The Manning's roughness coefficient (n) for conduits was estimated to be 0.03 (Rossman, 2017), and the Manning's n for impervious and pervious subcatchment areas were estimated to be 0.03 and 0.1, respectively (Brunner, 2021). Subcatchment percent imperviousness and CN were estimated using the Spatial Weighting tool once 2021 NLCD imperviousness and land cover raster datasets along with soil data from the Natural Resources Conservation Service (NRCS) Web Soil Survey were processed in ArcGIS Pro. The spatial weighting tool in PCSWMM averaged characterized pixel counts from the processed percent imperviousness and CN raster datasets and assigned values to each subcatchment shape. Due to the model scale and lack of modeled detailed infrastructure, subcatchment subarea routing was set for both impervious and pervious areas to flow directly to the subcatchment outlet rather than directing flow from pervious areas to impervious areas before reaching the outlet node.

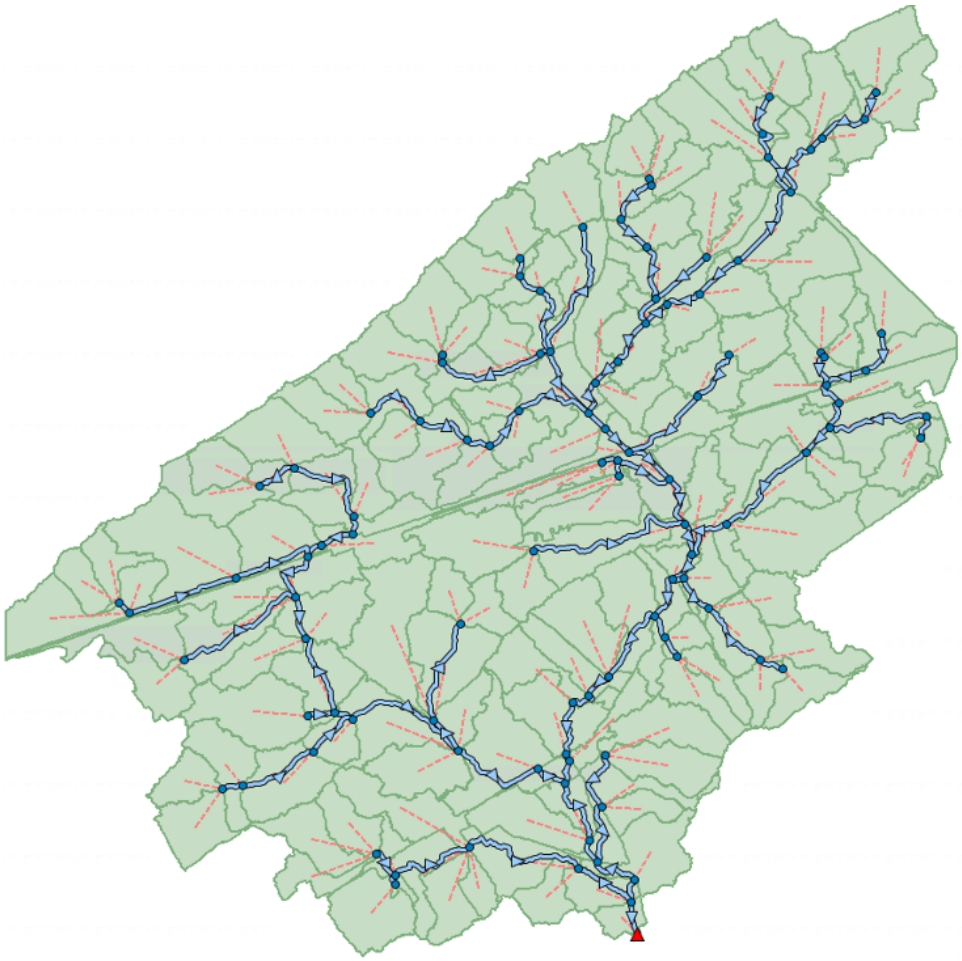


Figure 4: Model I

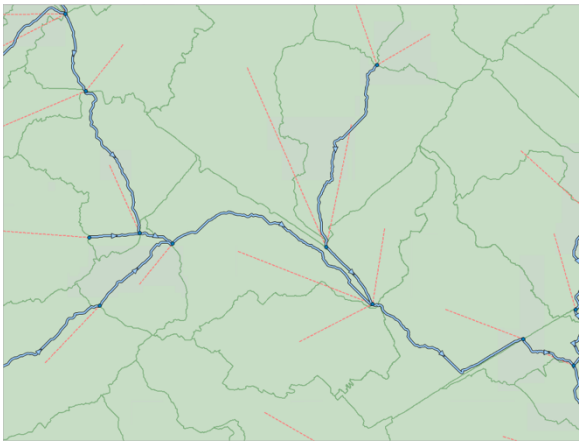


Figure 5: Magnified View of Model I

Default values were used for all other subcatchment parameters relating to infiltration and overland flow.

The calibration technique used for Model I involved adjusting node inflows, rainfall data, conduit Manning's n, subcatchment CN, subcatchment percent imperviousness, and subcatchment impervious area Manning's n. Modeled water depths at the most downstream conduit were compared to observed water depths from the adjacent TNWRRC monitoring gauge (Figure 2). Node inflows were adjusted using a stage-discharge relationship (Figure 3) and manual estimations of average observed depths influenced by seasonal variation. A monthly time pattern was created in the model that established seasonally varied baseflow. Rainfall data was adjusted to account for spatial and temporal variation, since the USGS Beaver Creek monitoring gauge is located approximately 18 kilometers northeast of the study site. Uncalibrated model output depths were compared to observed depths to calculate ratios that were applied to rainfall events. Additionally, modeled and observed depths were compared to add or remove storm events. The PCSWMM Sensitivity-based Radio Tuning Calibration (SRTC) tool was used to perform final calibration of the following parameters: conduit Manning's n, subcatchment CN, subcatchment percent imperviousness, subcatchment impervious area Manning's n, and baseflow. Only subcatchment CN, subcatchment percent imperviousness, and baseflow required adjustment during final calibration, and the resulting coefficient of determination (R^2) value of Model I equaled 0.725.

Model II

Model II was built using desktop data, automated PCSWMM tools, geomorphic-based node selection, and field verification to serve as a medium-developed model (Figures 6 and 7). The conveyance network was generated by the WDT using the same methodology as Model I. Conduits and nodes were manually adjusted to align with depressions in the DEM and approximate RGA locations. WDT-generated nodes were assigned elevations using the elevations from DEM tool. To represent geomorphic-based node selection, HGC nodes were manually added upstream and downstream of the Red Mill Dam and at approximate road and pedestrian crossings using aerial imagery, the DEM, and field notes taken when performing RGAs along main channel stems. The Set Invert tool was used to assign elevations to HGC nodes effectively cutting through high places

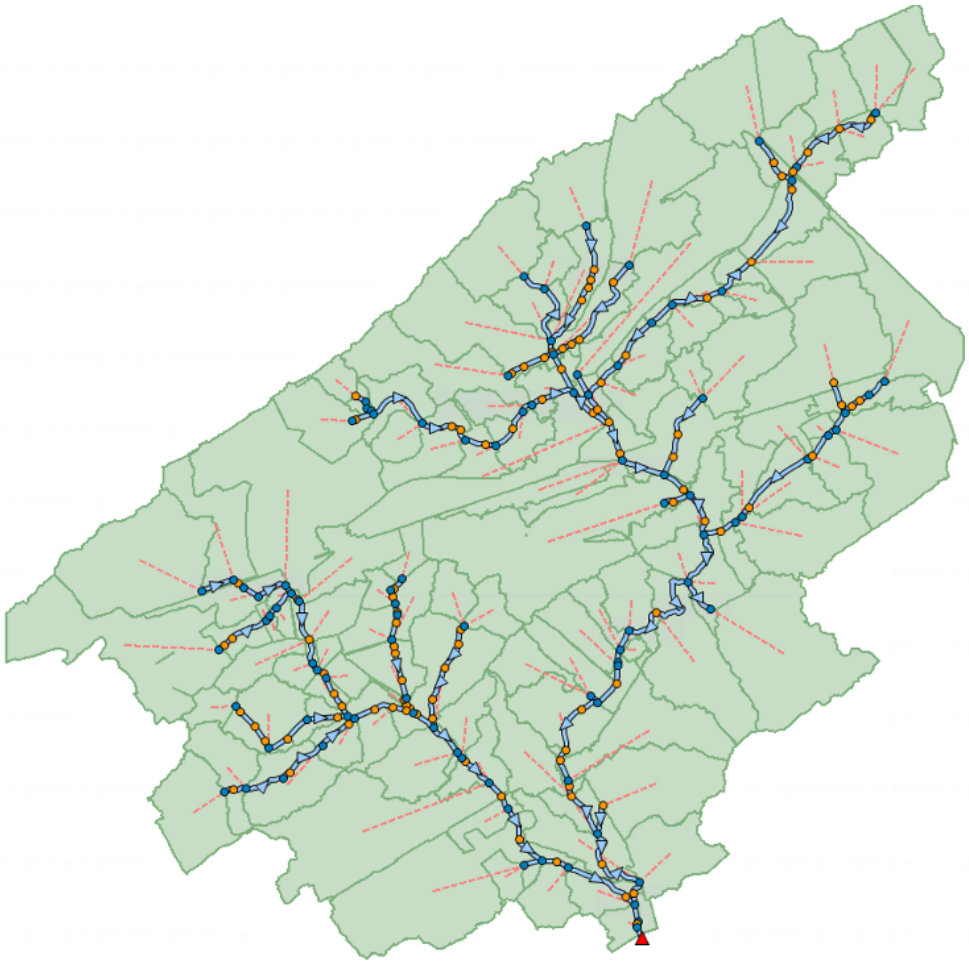


Figure 6: Model II

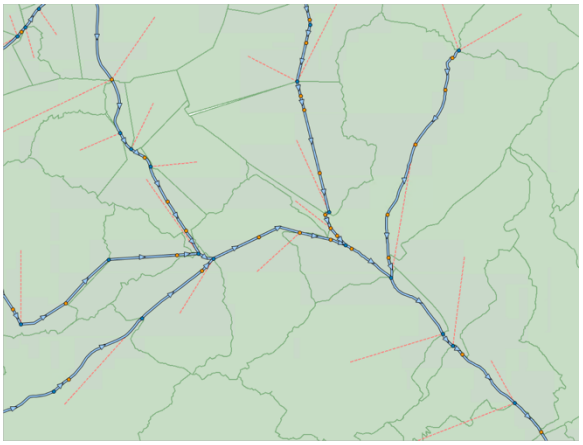


Figure 7: Magnified View of Model II

in the DEM by interpolating surrounding WDT-generated node elevations. Conduits slopes were reviewed to ensure none were adverse, and subcatchments were manually edited to account for roadway and infrastructure boundaries seen in aerial imagery, the DEM, and stormwater infrastructure spatial data provided by the Town of Farragut. Channel geometries were assigned to conduits using the same methodology as Model I. Near the downstream extent of the model, three transverse weirs surrounded by previously added HGC nodes were spliced into the conveyance network to mimic the Red Mill Dam's three breaches (Figure 8). Weirs were visually estimated to be 0.912 meters in height, 1.524 meters in length, and level with the ground. In plan view, weir shapes were drawn to be approximately 10 meters in length. The default discharge coefficient of 3.33 cubic meters per second was kept, and weirs were set to have surcharging capacity as enabled by the use of the dynamic wave routing method.

The calibration technique used for Model II was similar to that of Model I. The baseflow monthly time pattern and adjusted rainfall data used in Model I were input into Model II. The seasonally varied node baseflows were only added to WDT-generated nodes to avoid adding excessive inflows to the model. The SRTC tool was used to perform final calibration of the following parameters: conduit Manning's n, subcatchment CN, subcatchment percent imperviousness, and subcatchment impervious area Manning's n. Only subcatchment CN, subcatchment percent imperviousness, and subcatchment impervious area Manning's n required adjustment during final calibration. The adjusted impervious area Manning's n equaled 0.015, and the resulting R^2 value of Model II equaled 0.715.

Model III

Model III was built using desktop data, automated PCSWMM tools, geomorphic-based node selection, SCMs, and field verification to serve as a high-developed model (Figures 9 and 10). The conveyance network was generated by the WDT using the same methodology as Model I. Using the same methodology as Model II, conduits and nodes were manually adjusted, and HGC nodes were added. Stormwater ponds were added to Model III as storages using the Storage Creator tool. The tool first created storage polygons based on a fill pits operation on the DEM. The minimum requirements for a polygon to be drawn were a depth of 1 meter and an area of 100 square meters.



Figure 8: Red Mill Dam

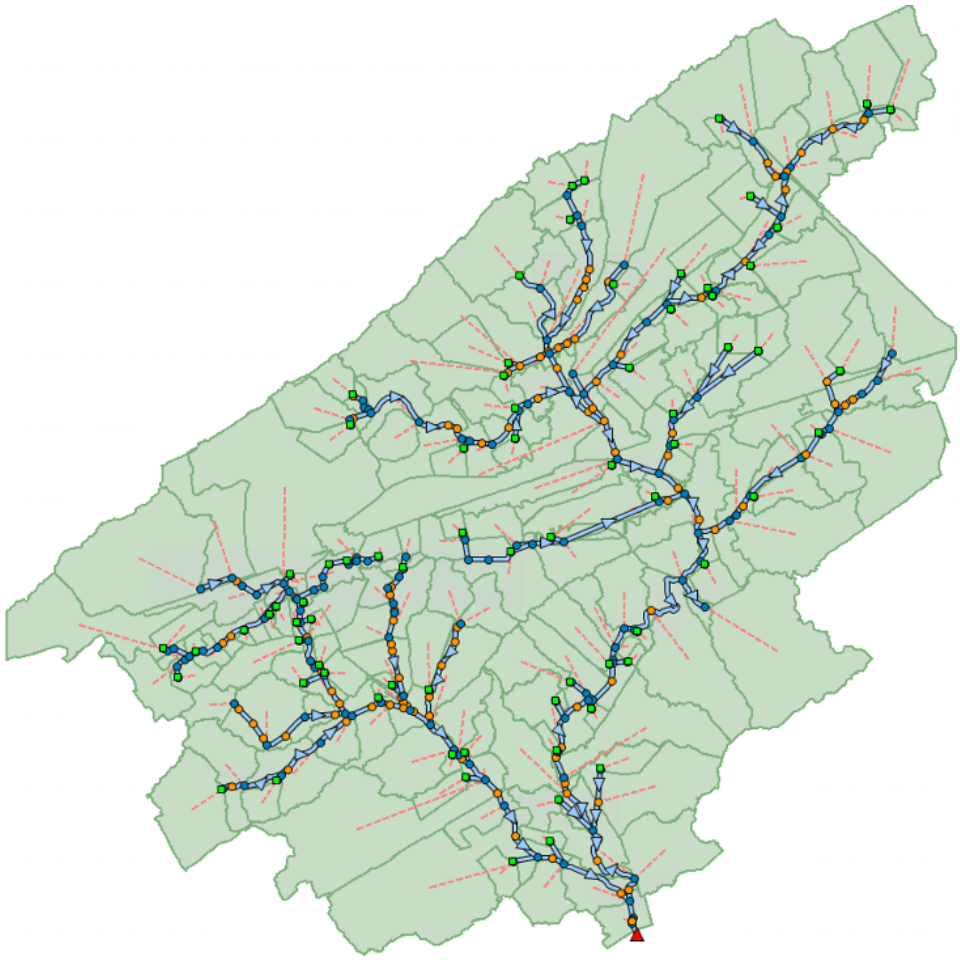


Figure 9: Model III



Figure 10: Magnified View of Model III

The tool then generated storages and storage curves using the DEM, storage polygon layer, and elevation interval of 0.25 meters. The maximum height of storage curves was set to the minimum perimeter (spill) elevation, and the corresponding storage unit invert elevation was set to equal the lowest sampled DEM elevation. Aerial imagery and the DEM were used to manually add or remove stormwater ponds. Due to a lack of stormwater infrastructure data, ponds were added using a representative storage curve. The additional storages were assigned invert elevations by subtracting the depth of the representative storage curve from the rim elevations assigned using the elevations from DEM tool. Transverse weirs with bounding nodes were connected to all storages. Bounding nodes were assigned the same invert elevation as storages to set weir slopes at 0 percent. Based on field reconnaissance, weirs were estimated to be 0.1524 meters in length and level with the ground (Figure 11). Weir height was estimated to be 0.61 meters less than the pond rim elevation minus the invert elevation (Tschantz, Gangaware, & Morton, 2003). Additionally, weir shapes were drawn in plan view to be approximately 1.524 meters in length. The default discharge coefficient of 3.33 cubic meters per second was kept, and weirs were set to have no surcharging capacity due to the absence of vertical limitation. To connect storages, weirs, and bounding nodes to the conveyance network, additional conduits were added as either circular pipes or open swales. Based on stormwater pipes spatial data provided by the Town of Farragut, circular pipes were set to be 0.61 meters in diameter with a Manning's n of 0.01 (Rossman, 2017). Aerial imagery, the DEM, and stormwater infrastructure spatial data were used to determine the type of drainage feature needed and where that feature should outlet on the conveyance network. Additionally, subcatchments were manually edited to route to storages or WDT-generated nodes and account for roadway and infrastructure boundaries. Three transverse weirs and surrounding HGC nodes were included to represent the Red Mill Dam's breaches using the same methodology as Model II. Once the conveyance network was finalized, the elevations from DEM tool was used to assign WDT-generated node elevations. HGC node elevations were also set using the Set Invert tool. Conduit slopes were checked to ensure none were adverse, and cross-sectional channel geometries were applied to open channels using the same methodology as Model I.

The calibration technique used for Model III was similar to that of Model I and Model II, and the only differences between Model II and Model III were the SRTC calibration results. The baseflow



Figure 11: Example Outlet Structure in Turkey Creek Watershed

monthly time pattern and adjusted rainfall data used in the other models were input into Model III, and the seasonally varied node baseflows were only added to WDT-generated nodes to avoid adding excessive inflows to the model. The SRTC tool was used to perform final calibration of the following parameters: conduit Manning's n, subcatchment CN, subcatchment percent imperviousness, and subcatchment impervious area Manning's n. All variables required adjustment during final calibration. The adjusted impervious area Manning's n equaled 0.015, and conduit roughness for open channels and pipes changed to 0.0441 and 0.0147, respectively. The resulting R^2 value of Model III equaled 0.735.

Geomorphic/Model Analysis

Stream Power and Bed Shear Stress Determination for Model Reaches

Maximum conduit discharge (Q_{max}), hydraulic radius (R_{max}), and conduit slope (S) were exported from each PCSWMM model simulation to calculate the maximum bed shear stress (τ_{max}, Eq. 1) and stream power (Ω_{max}, Eq. 2) experienced by each conduit. Flow rates and geometry were obtained from the 10-year simulation. To qualitatively compare model simulations across the watershed, model conduits were analyzed rather than the 19 geomorphic-based analysis reaches that only represent main channel segments. The specific weight of water (γ) equaled 9,810 newtons per cubic meter, and energy slope was approximated as channel slope.

$$\tau_{max}\,(\text{Pa}) = \gamma R_{max} S \qquad (1)$$

$$\Omega_{max}\,(\text{W/m}) = \gamma Q_{max} S \qquad (2)$$

Model conduits were exported from PCSWMM and imported to ArcGIS Pro to allow for visual representation of τ_{max} and Ω_{max} values. The values were added as additional fields, and conduit symbology was set to display graduated colors based on each parameter.

Percentile Stream Power and Bed Shear Stress Determination for Analysis Reaches

For each model simulation, 30th, 50th, and 80th-percentile bed shear stress ($\tau_{30,50,80}$, Eq. 3) and stream power ($\Omega_{30,50,80}$, Eq. 4) calculations were performed for the 19 geomorphic-based analysis reaches determined during field investigation. The 19 analysis reaches were drawn in ArcGIS Pro

and compared to model conduits to compile a list showing which conduits overlapped each analysis reach. The effective lengths of model conduits overlapping analysis reaches were measured and used to calculate length-weighted averages of depth and discharge at each model time step of 1 hour. These discharge and depth values were then used to determine the percentile depth ($D_{30,50,80}$) and discharge ($Q_{30,50,80}$) of each analysis reach. For $\tau_{30,50,80}$ calculations, hydraulic radius was approximated to equal conduit depth, since PCSWMM does not provide continuous hydraulic radius data. Analysis reach slope (S_{avg}) was used to approximate energy slope and determined by averaging model conduit slopes, and the specific weight of water (γ) equaled 9,810 newtons per cubic meter.

$$\tau_{30,50,80}\,(\text{Pa}) = \gamma D_{30,50,80} S_{avg} \qquad (3)$$

$$\Omega_{30,50,80}\,(\text{W/m}) = \gamma Q_{30,50,80} S_{avg} \qquad (4)$$

Resulting values of $\tau_{30,50,80}$ and $\Omega_{30,50,80}$ were used to perform single regression analyses and stepwise linear multiple regression analyses as described in the following sections.

Single Regression Analysis

Based on analysis reach data, single regression analyses, which included analysis of variance (ANOVA) tests, were performed for each model simulation using Microsoft Excel with the independent variable set as the RGA score and dependent variable set as $\tau_{30,50,80}$ or $\Omega_{30,50,80}$. Modeled R^2, significance (P), variance ratio (F), and variance significance (F_{sig}) values were used to compare regression results. Additionally, $\tau_{30,50,80}$ and $\Omega_{30,50,80}$ values were plotted against RGA scores to visualize the relationship among variables.

Stepwise Linear Multiple Regression Analysis

Using Statistical Package for Social Sciences (SPSS) Statistics and analysis reach data, stepwise linear multiple regression analyses, which included ANOVA tests, were performed for each model simulation to determine which of the following independent variables best predict $\tau_{30,50,80}$ and $\Omega_{30,50,80}$: RGA score, all RGA sub-metrics, drainage area, S_{avg}, urban and forested land use percentages above reach, and average, longest, and shortest distances between HGCs. All

regression models were performed twice with and without including drainage area and S_{avg} as independent variables, since both variables are directly related to discharge, flow depth, and energy slope (Lea & Legleiter, 2016; Vocal Ferencevic & Ashmore, 2012). Additionally, probabilities of 0.3 and 0.4 were used as stepping method entry and exit limits, respectively. RGA score was input into the model as ordinal data, RGA sub-metrics were input as nominal data, and all other independent variables were input as scale data.

Independent variables used in regression analyses other than RGA score, RGA sub-metrics, and S_{avg} were determined using a both PCSWMM and ArcGIS Pro. Drainage areas were calculated by importing analysis reach breaks into PCSWMM, using the Rename Entities tool to identify subcatchments draining to the node nearest to a given reach break, and summing subcatchment areas in ArcGIS Pro. Urban and forested land use percentages above each reach were determined by dissolving subcatchments from PCSWMM into single polygons and generating pixel-count summaries for each polygon using the 2021 NLCD land cover raster dataset. Average, longest, and shortest distances between HGCs were manually measured in ArcGIS Pro by importing HGC nodes from PCSWMM and tracing analysis reach lines between nodes. Distances between HGCs were the same across model simulations, since HGC nodes were identical in Model II and Model III and not included in Model I. Regression model R^2, F, and F_{sig} values and P values of statistically significant independent variables were used to compare results.

CHAPTER THREE
RESULTS

Watershed Reach Determination/Designation

The 19 geomorphic-based analysis reaches were visualized in Figure 1. Identified major hydraulic grade controls (HGCs) included road crossings, a natural beaver dam between rapid geomorphic assessments (RGAs) 16 and 17, and the Red Mill Dam. Analysis reach breaks were mostly represented as locations of HGCs with the exception being the confluence of Turkey Creek and North Fork Turkey Creek. Additionally, reaches 10 and 11 were split due to a change in land use but shared the same RGA score, since a separate RGA was not performed for reach 10 during field reconnaissance.

Rapid Geomorphic Assessment (RGA) Scores

Resulting RGA scores for designated analysis reaches were summarized in Table 1, and an example RGA form was included in Figure 12. Most reaches scored as either moderately stable or instable with only reaches 1, 3, and 5 scoring as stable. The average RGA score equaled 17.8 suggesting moderate channel instability in the overall study watershed. Additionally, the average stage of channel evolution of 3 represented the degradation of analysis reaches in the field.

Model Reach Maximum Stream Power and Bed Shear Stress Maps

For each model simulation, maps were created in ArcGIS Pro to either visualize model conduit maximum bed shear stress (τ_{max}) or maximum stream power (Ω_{max}) (Figures 13 through 18, Attachment B). Model I τ_{max} values ranged from -2,317.4 to 4,428.2 pascals, and Ω_{max} values ranged from -2,016.8 to 13,685.3 watts per meter. Negative results were caused by adverse slopes in Model I. Model II τ_{max} and Ω_{max} values ranged from 2.6 to 2,922 pascals and 34.0 to 130,800.3 watts per meter, respectively. Model III τ_{max} values ranged from 0.9 to 6,939.2 pascals, and Ω_{max} values ranged from 4.1 to 101,872.4 watts per meter. Adverse slopes were manually removed from Models II and III which prevented negative calculations. Despite varying ranges and negative

Table 1: RGA Scores

RGA Number/Metric	1	2	3	4	5	6	7	8	9	10	11	12	13	14	15	16	17	18
Applicable Analysis Reach	1	2	3	4	5	6	7	8	9	10/11	12	13	14	15	16	17	18	19
Total Score	9.5	21.5	10.5	18.5	6	17.5	19.5	18.5	23.5	20.5	17.5	16.5	16	18.5	23	22	16	23
Primary Bed Material	0	1	1	2	0	0.5	0.5	1	4	0.5	1	2	2	4	4	4	4	4
Bed/Bank Protection	1	1	0	1	0	1	1	1	1	1	1	1	1	1	1	1	1	1
Degree of Incision	0	2	2	2	1.5	1	2	2	4	0	2	0	0	2	3	1	0	0
Degree of Constriction	0	1	0	0	0	0	1	0	1	0	0	0	0	2	0	0	0	0
Stream Bank Erosion (Left Bank)	1	2	0	2	1	1	2	2	2	2	2	2	2	1	2	2	1	2
Stream Bank Erosion (Right Bank)	1	2	2	2	1	2	2	2	2	2	2	2	2	1	2	2	1	2
Stream Bank Instability (Left Bank)	0	2	0	2	0	0	2	0.5	1.5	2	1	2	0.5	0	1	1.5	0	2
Stream Bank Instability (Right Bank)	0	2	0.5	1.5	0	1	1	1.5	1	2	1	2	1.5	0	1	1.5	0	2
Established Riparian Woody-Vegetative Cover (Left Bank)	0.5	1	0	0.5	0.5	2	2	1	0.5	1.5	0.5	1	1	1.5	1	1	1.5	1
Established Riparian Woody-Vegetative Cover (Right Bank)	0.5	1.5	0	0.5	0.5	2	0.5	1	0.5	1.5	0.5	0.5	0.5	1.5	1	1	1.5	1
Occurrence of Bank Accretion (Left Bank)	2	1.5	2	1	0	2	2	2	1.5	2	1.5	0.5	0.5	1	2	1.5	1	2
Occurrence of Bank Accretion (Right Bank)	2	1.5	2	1	0	2	0.5	1.5	1	2	1.5	0.5	2	2	2	1.5	1	2
Stage of Channel Evolution	1.5	3	1	3	1.5	3	3	3	3.5	4	3.5	3	3	1.5	3	4	4	4

Lat/Long ≈ 35.8722, -84.4487

CHANNEL-STABILITY RANKING SCHEME

River T.C. Site Identifier Behind Red Mill Dam

Date 6/28/2023 Time 09:00 Crew _____ Samples Taken _____

Pictures (circle) U/S D/S X-section Slope _____ Pattern: Meandering Straight Braided

1. Primary bed material

Bedrock	Boulder/Cobble	Gravel	Sand	Silt Clay	
0	(1)	2	3	4	1

2. Bed/bank protection

Yes	No	(with)	1 bank protected	2 banks	
0	(1)		2	3	1

3. Degree of incision (Relative elevation of "normal" low water; floodplain/terrace @ 100%)

0-10%	11-25%	26-50%	51-75%	76-100%	
4	3	(2)	1	0	2

4. Degree of constriction (Relative decrease in top-bank width from up to downstream)

0-10%	11-25%	26-50%	51-75%	76-100%	
0	(1)	2	3	4	1

5. Stream bank erosion (Each bank)

	None	Fluvial	Mass wasting (failures)	
Left	0	1	(2)	2
Right	0	1	(2)	2

6. Stream bank instability (Percent of each bank failing)

	0-10%	11-25%	26-50%	51-75%	76-100%	
Left	0	0.5	1	1.5	(2)	2
Right	0	0.5	1	1.5	(2)	2

7. Established riparian woody-vegetative cover (Each bank)

	0-10%	11-25%	26-50%	51-75%	76-100%	
Left	2	1.5	(1)	0.5	0	1
Right	2	(1.5)	1	0.5	0	1.5

8. Occurrence of bank accretion (Percent of each bank with fluvial deposition)

	0-10%	11-25%	26-50%	51-75%	76-100%	
Left	2	(1.5)	1	0.5	0	1.5
Right	2	(1.5)	1	0.5	0	1.5

9. Stage of channel evolution

I	II	III	IV	V	VI	
0	1	2	4	(3)	1.5	3

Figure 1 – Channel stability ranking scheme used to conduct rapid geomorphic assessments (RGAs). The channel stability index is the sum of the values obtained for the nine criterion.

Σ 21.5

Figure 12: Example RGA

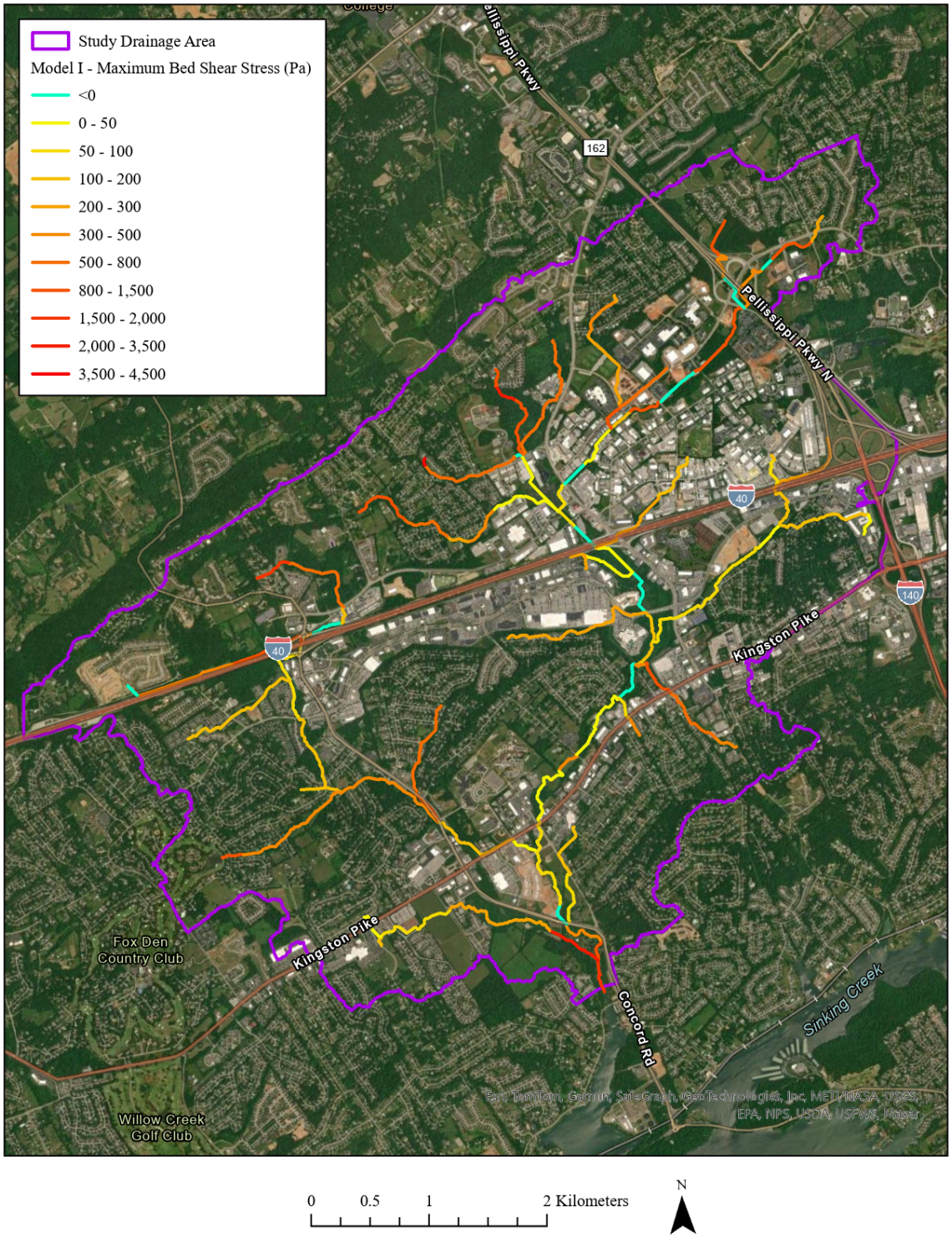


Figure 13: Model I Maximum Bed Shear Stress Map

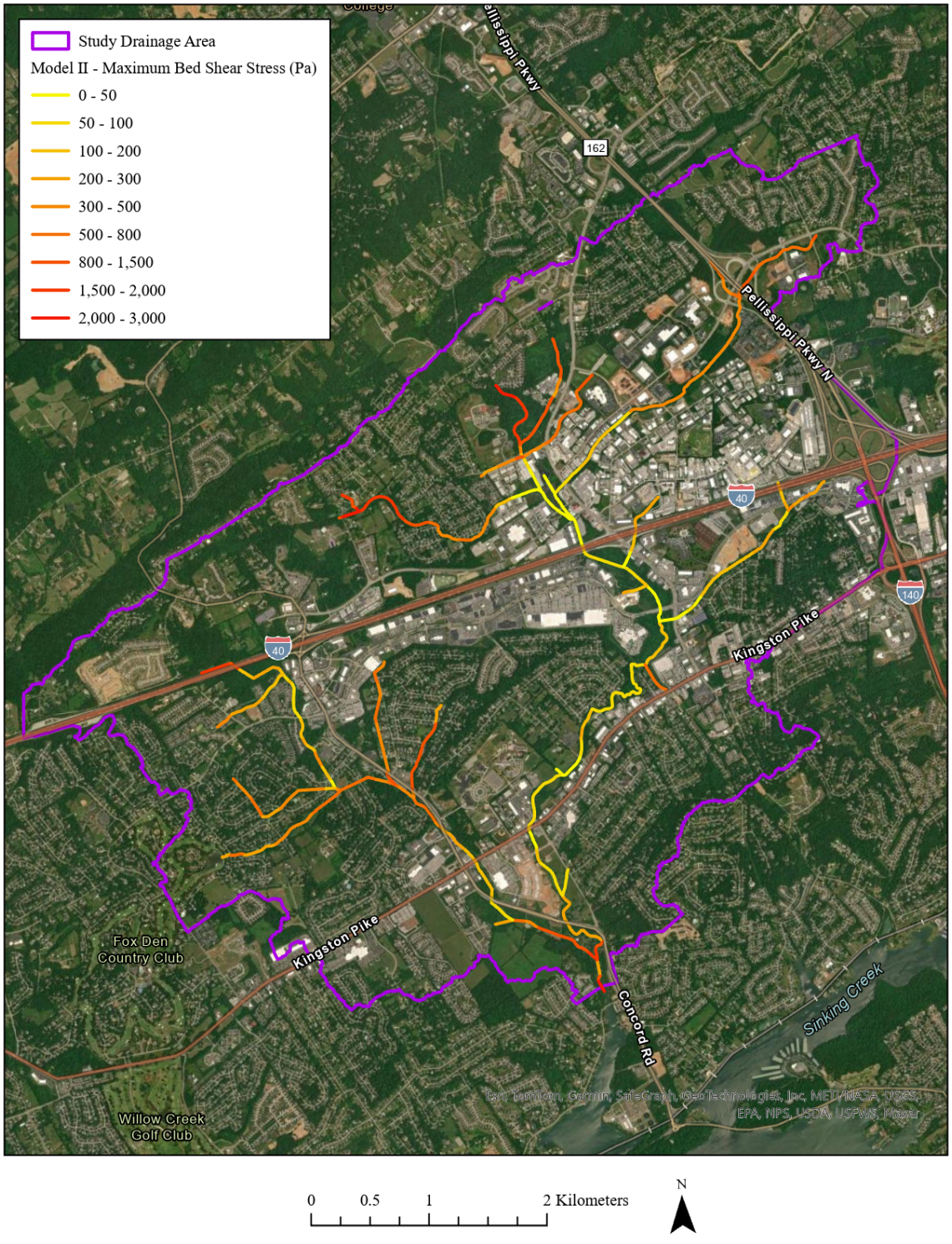


Figure 14: Model II Maximum Bed Shear Stress Map

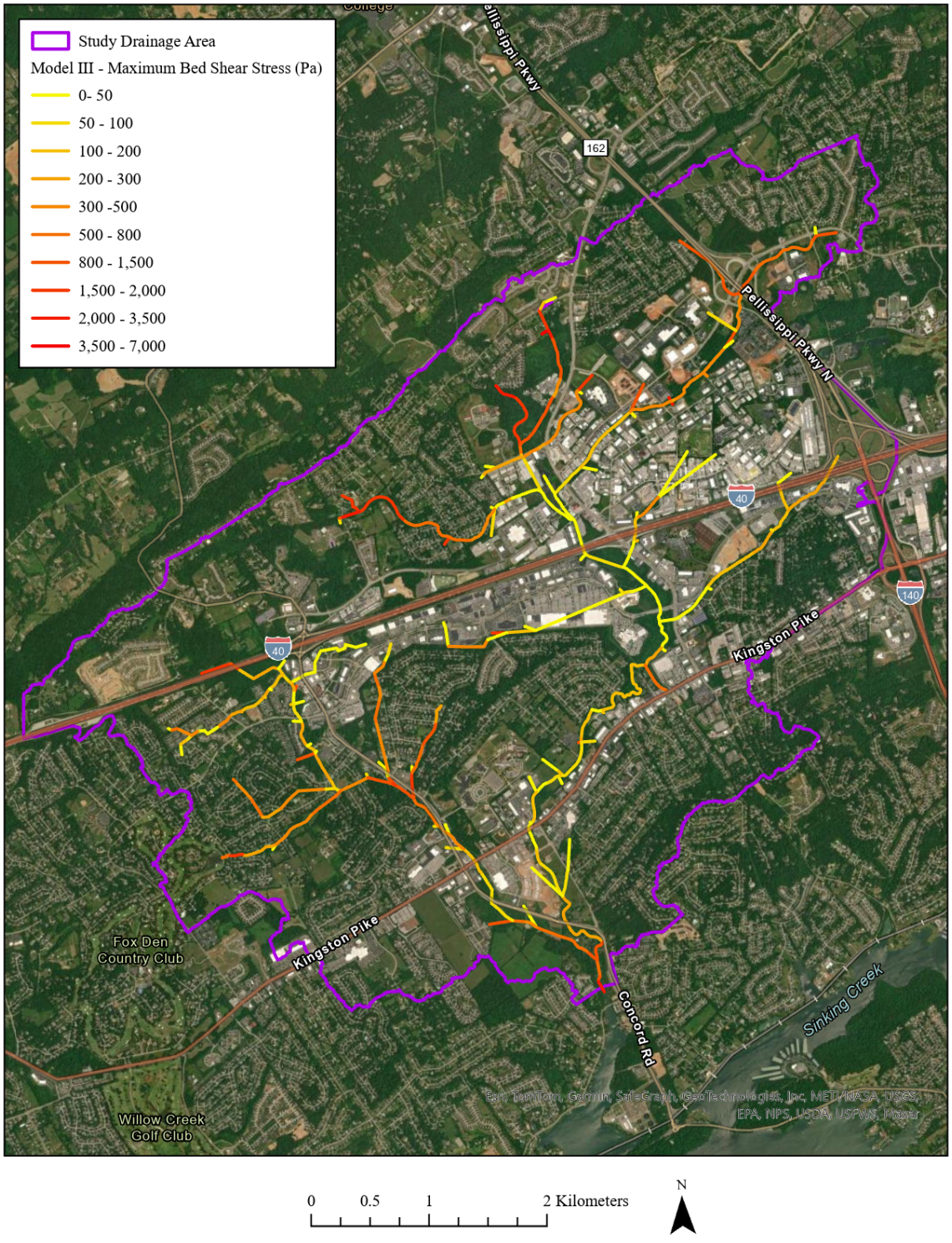


Figure 15: Model III Maximum Bed Shear Stress Map

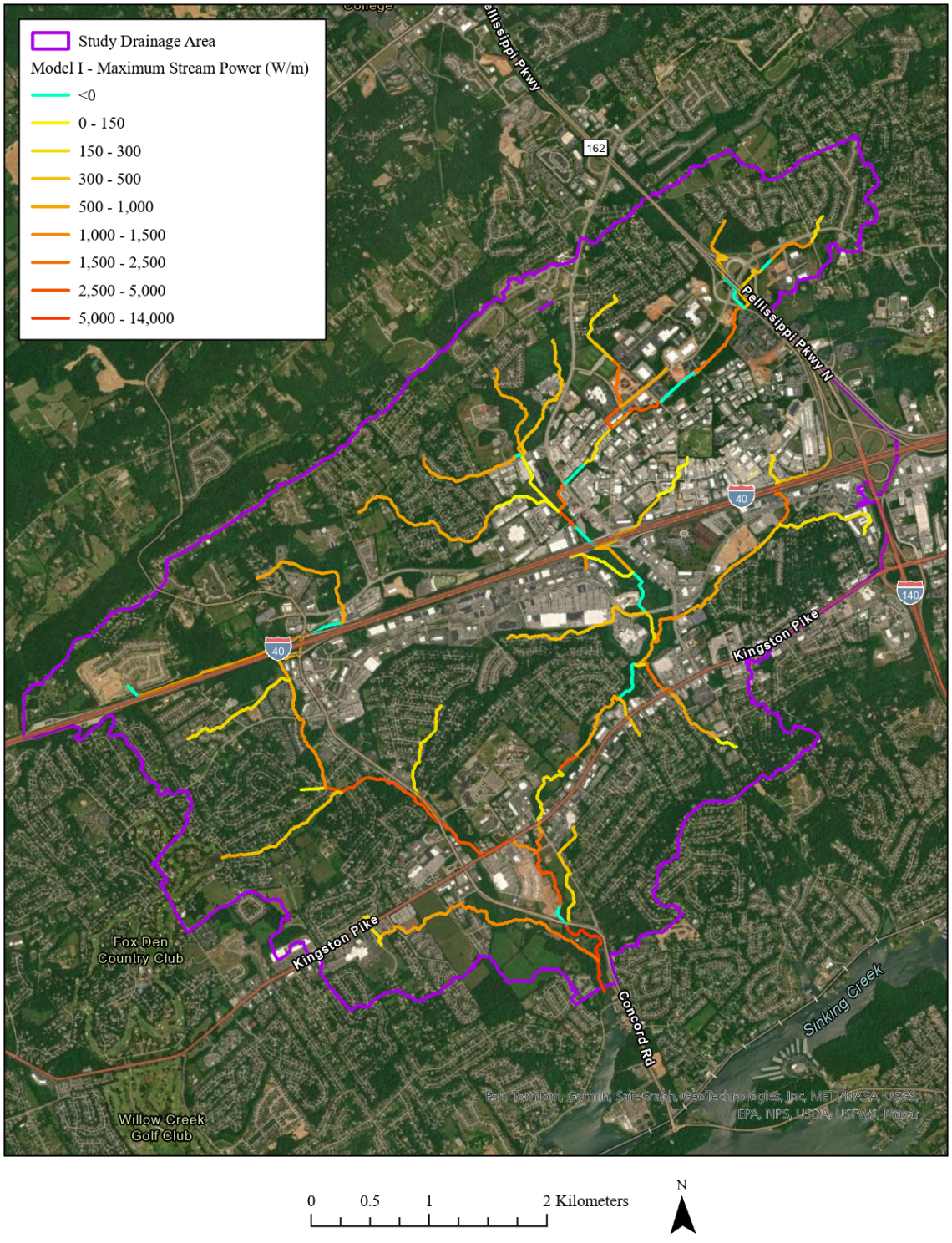


Figure 16: Model I Maximum Stream Power Map

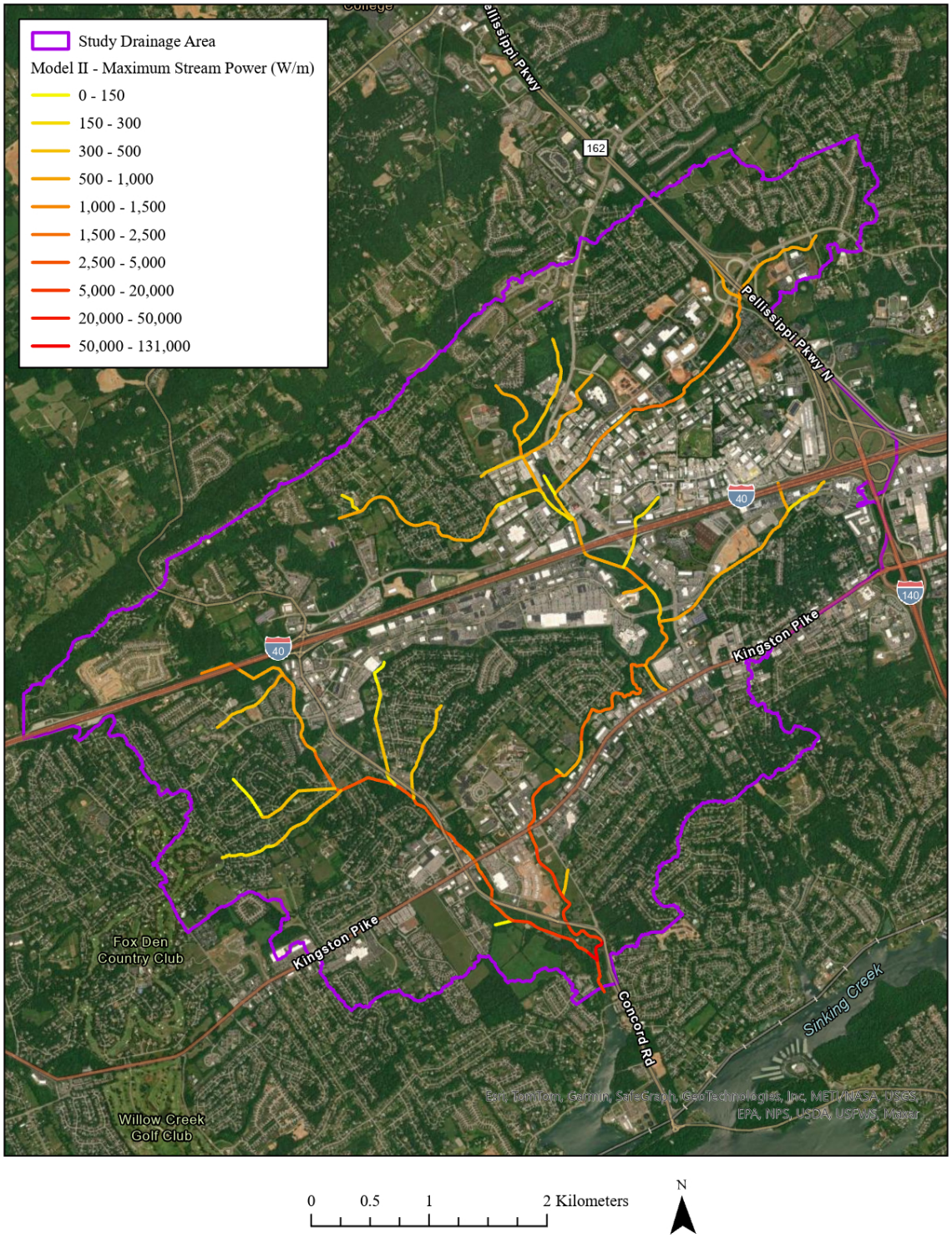


Figure 17: Model II Maximum Stream Power Map

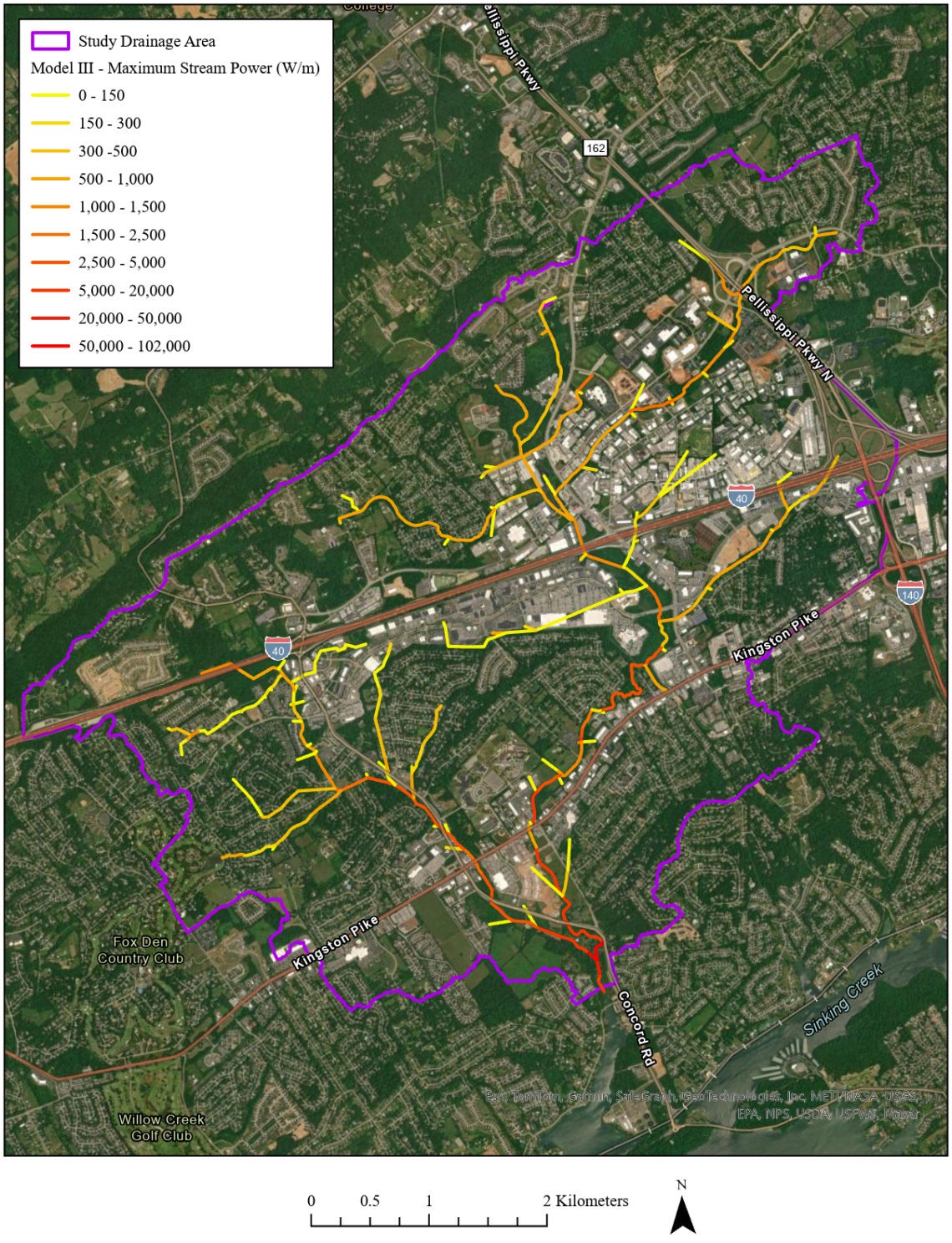


Figure 18: Model III Maximum Stream Power Map

Model I values, τ_{max} and Ω_{max} averages were relatively consistent among model simulations. τ_{max} averages equaled 407.0, 452.9, and 434.0 pascals for Model I, Model II, and Model III, respectively. Similarly, for Ω_{max}, averages equaled 1,132.4, 2,945.9, and 1,892.9 watts per meter.

Single Regression Analysis Results

Percentile stream power ($\Omega_{30,50,80}$) and bed shear stress ($\tau_{30,50,80}$) values were included in Table 2 along with corresponding analysis reaches and RGA scores. To assess the correlation between RGA score and $\Omega_{30,50,80}$ as well as RGA score and $\tau_{30,50,80}$, respective plots were created for each model simulation (Figures 19 through 24). Results from single regression analyses, which included analysis of variance (ANOVA) test results, were listed in Table 3 as the coefficient of determination (R^2), significance (P), variance ratio (F), and variance significance (F_{sig}) of each scenario. R^2 values ranged from 0.010 to 0.194, P values ranged from 0.059 to 0.677, and F values ranged from 0.180 to 4.102. F_{sig} and P values were identical, since only one independent variable was analyzed. For each single regression analysis, Models II and III yielded significantly higher R^2 and F values and lower P values as compared to Model I. Generally, the highest R^2 and F values and lowest P values were produced by Model III. With the exception of Model I, $\tau_{30,50,80}$ analyses yielded improved results moving from 30^{th} to 80^{th}-percentiles. Alternatively, $\Omega_{30,50,80}$ analyses results were generally consistent among percentiles.

Stepwise Linear Multiple Regression Analysis Results

Results from stepwise linear multiple regression analyses, which included ANOVA test results, were tabulated per model simulation for $\Omega_{30,50,80}$ and $\tau_{30,50,80}$. Multiple regression models not including drainage area and slope as independent variables (exclusive) were included in Tables 4 through 9, whereas models including drainage area and slope (inclusive) were included in Tables 10 through 15. R^2, F, and F_{sig} values were compared for each model simulation along with P values of statistically significant independent variables grouped by the regression model. Additionally, tabulated independent variables were listed in the order of introduction into the regression model.

Table 2: Percentile Bed Shear Stress and Stream Power per Analysis Reach

	Analysis Reach	1	2	3	4	5	6	7	8	9	10	11	12	13	14	15	16	17	18	19
	RGA Score	9.5	21.5	10.5	18.5	6	17.5	19.5	18.5	23.5	20.5	20.5	17.5	16.5	16	18.5	23	22	16	23
Model I	τ_{30} (Pa)	48.9	48.9	18.5	35.4	17.1	14.7	17.6	17.6	12.0	9.2	6.2	18.4	10.6	9.6	15.6	13.6	9.0	29.2	42.6
	τ_{50} (Pa)	54.0	54.0	20.5	38.6	18.4	16.7	20.6	20.6	14.0	10.7	7.2	19.5	11.2	10.1	16.1	15.1	10.3	33.4	47.7
	τ_{80} (Pa)	59.3	59.3	22.6	41.8	19.8	18.9	23.6	23.6	16.0	12.2	8.2	20.8	11.8	10.5	16.4	16.5	11.4	37.0	52.1
	Ω_{30} (W/m)	311.5	311.5	9.4	158.5	50.5	27.0	28.4	28.4	17.9	11.6	6.8	38.8	27.8	14.2	21.3	22.5	7.9	25.9	23.7
	Ω_{50} (W/m)	381.6	381.6	12.8	192.1	59.7	36.7	38.7	38.7	24.3	15.8	9.3	43.9	31.1	15.7	24.0	30.5	10.7	34.7	32.0
	Ω_{80} (W/m)	460.9	460.9	16.8	230.2	70.5	48.2	50.4	50.4	31.7	20.5	12.0	50.0	35.2	17.5	26.9	38.8	13.5	43.8	41.0
Model II	τ_{30} (Pa)	39.1	15.9	20.5	12.2	14.7	13.5	10.3	4.4	4.9	35.8	20.6	12.5	15.6	10.3	7.8	7.5	8.7	10.5	8.8
	τ_{50} (Pa)	45.3	17.5	23.5	14.1	17.1	15.7	11.9	5.2	5.6	41.3	24.0	14.6	18.2	12.0	9.1	8.3	10.1	12.3	10.3
	τ_{80} (Pa)	53.4	20.0	26.7	16.1	19.7	18.0	13.8	6.1	6.5	46.3	26.9	16.4	20.4	13.5	10.4	9.1	11.5	14.0	11.8
	Ω_{30} (W/m)	298.2	100.7	51.8	26.0	29.4	24.5	13.5	7.5	3.2	175.1	87.9	44.0	48.3	32.5	19.9	12.1	12.2	13.0	11.9
	Ω_{50} (W/m)	403.8	136.4	69.6	34.9	39.6	33.0	18.2	10.2	4.4	239.2	120.6	60.4	66.4	44.8	27.1	16.3	16.5	17.6	16.1
	Ω_{80} (W/m)	520.7	175.8	92.4	46.2	52.6	44.0	24.7	13.8	6.1	304.6	153.5	77.0	84.7	57.1	35.1	21.2	21.3	22.8	20.8
Model III	τ_{30} (Pa)	40.1	28.0	19.9	13.7	16.8	14.9	10.9	5.8	4.5	33.5	15.8	18.9	14.1	14.1	7.0	7.5	8.6	10.1	11.0
	τ_{50} (Pa)	44.7	30.9	22.7	15.7	19.4	17.1	12.5	6.7	5.2	37.0	17.4	22.0	16.4	16.3	7.9	8.5	10.0	11.8	12.2
	τ_{80} (Pa)	51.4	33.6	25.4	17.7	22.1	19.3	14.2	7.6	6.0	40.7	19.1	24.7	18.5	18.6	8.9	9.3	11.3	13.6	13.5
	Ω_{30} (W/m)	316.8	152.9	54.3	29.7	36.2	29.1	14.5	5.5	3.9	161.6	64.9	72.7	43.9	49.6	17.9	11.8	12.0	13.9	12.3
	Ω_{50} (W/m)	396.6	191.5	73.3	40.0	48.8	39.3	19.6	7.3	5.3	220.8	80.0	99.8	60.2	67.8	24.4	16.0	16.3	18.8	16.7
	Ω_{80} (W/m)	493.8	238.5	95.6	51.8	63.2	51.0	25.4	9.6	6.9	281.1	97.7	128.6	77.8	88.0	31.9	20.9	21.1	24.5	21.6

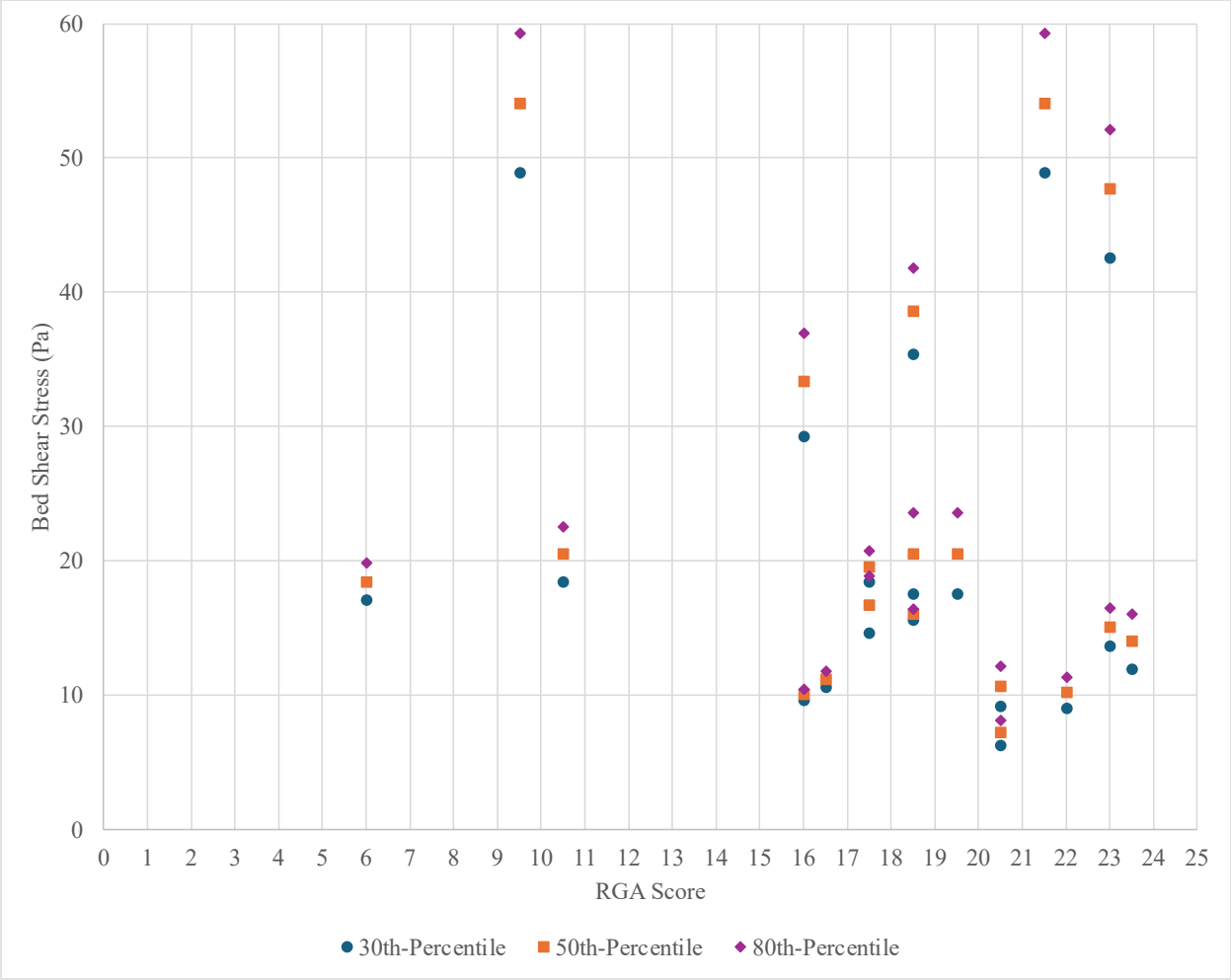


Figure 19: Model I Relationship Between RGA Score and Percentile Bed Shear Stress

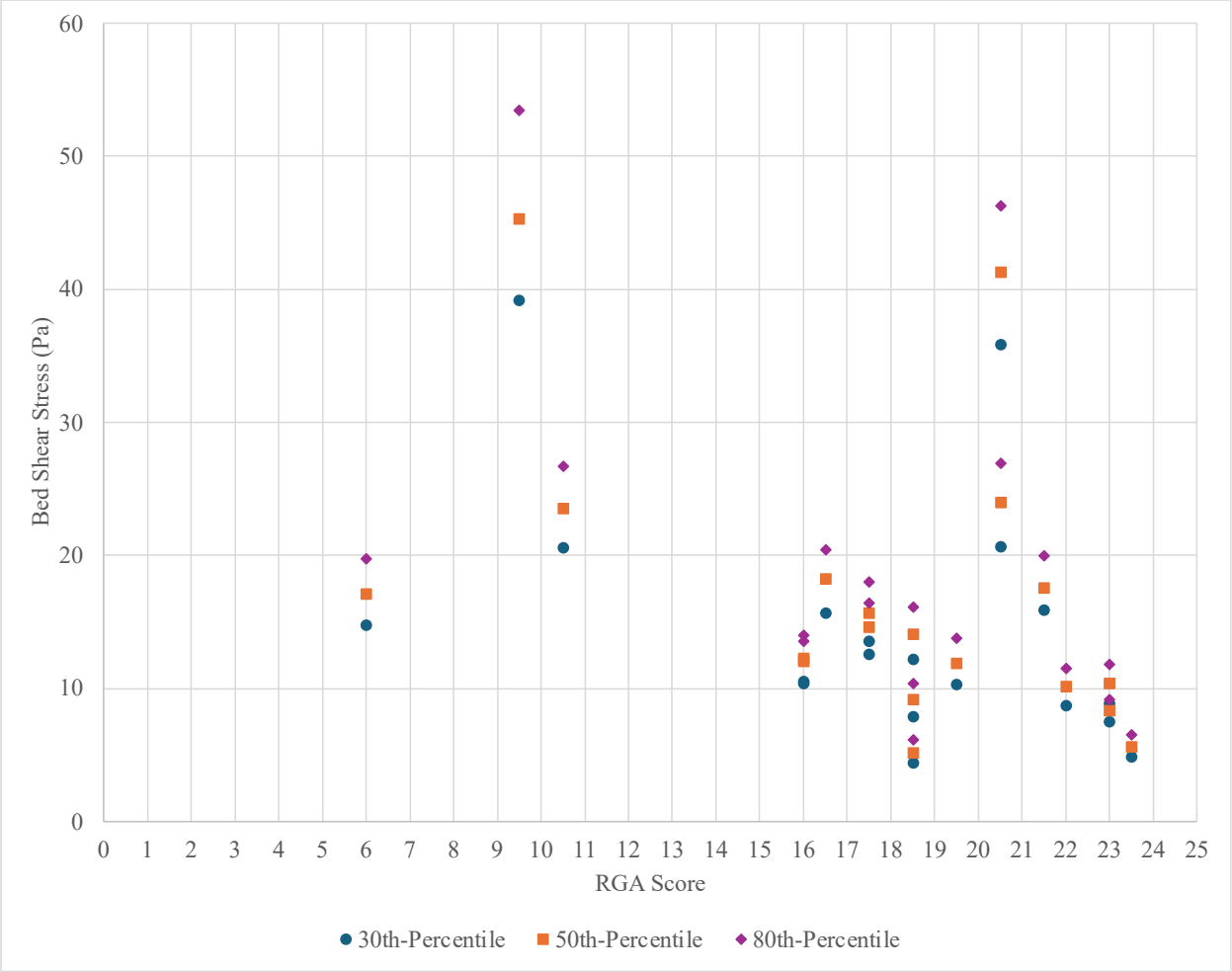


Figure 20: Model II Relationship Between RGA Score and Percentile Bed Shear Stress

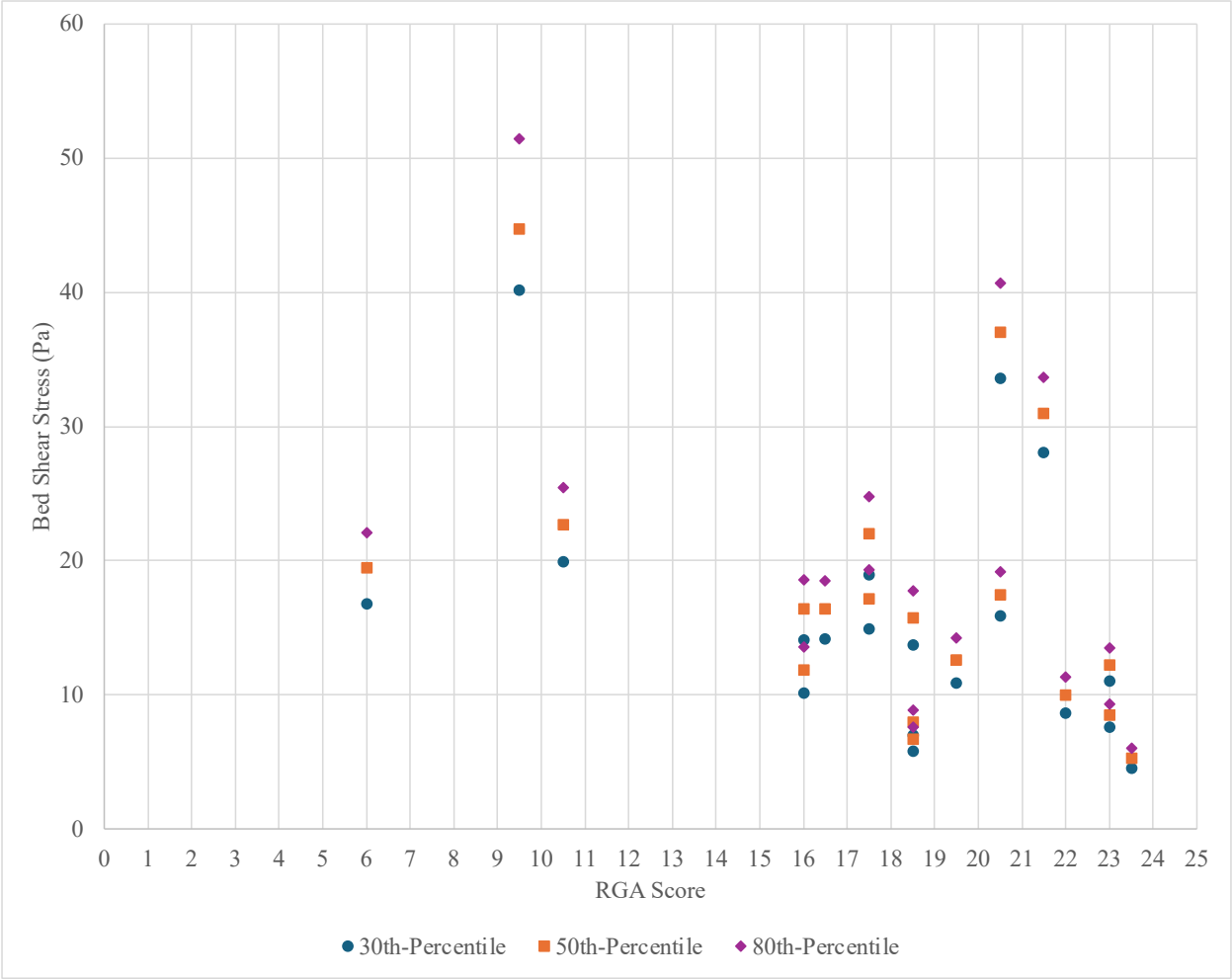


Figure 21: Model III Relationship Between RGA Score and Percentile Bed Shear Stress

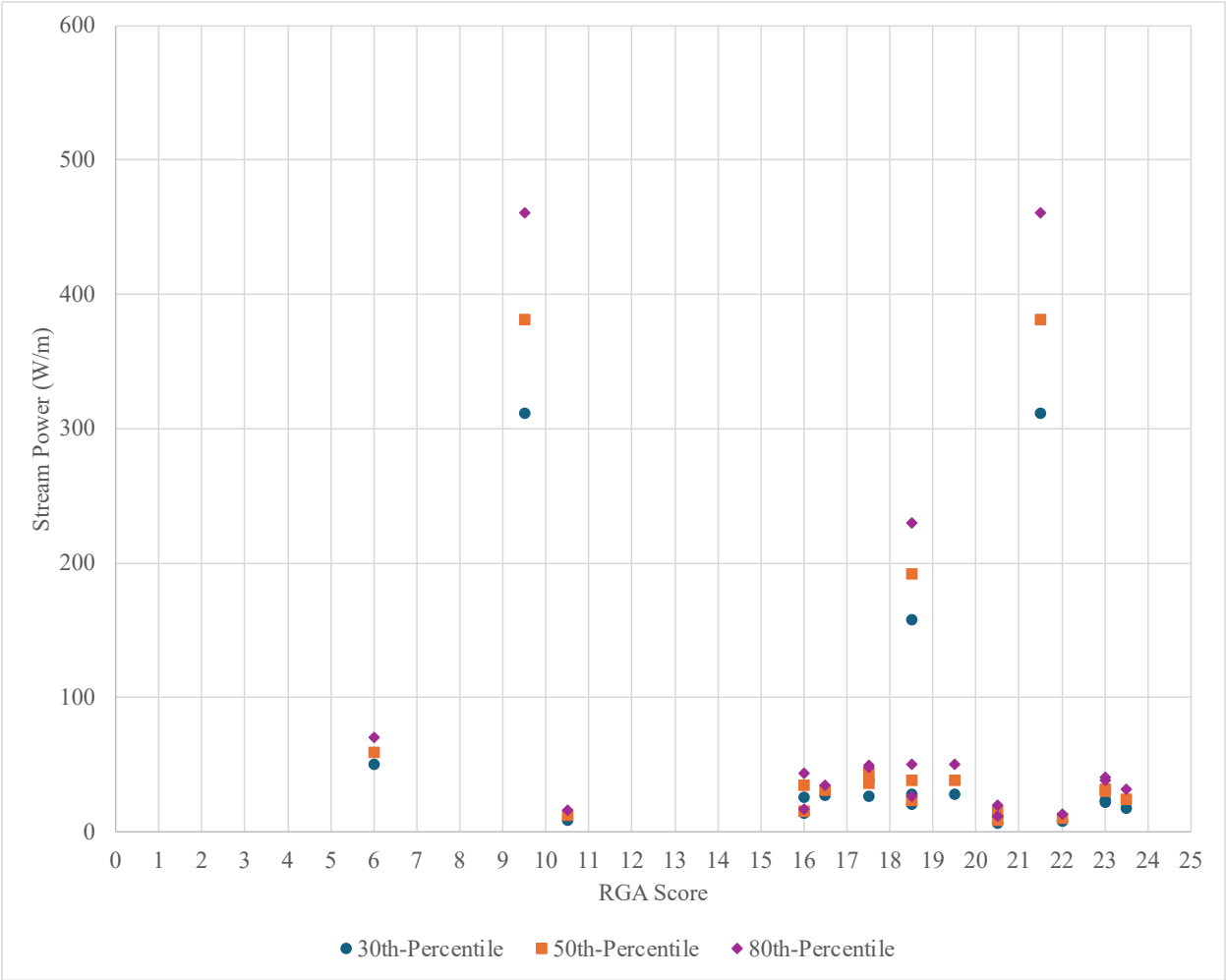


Figure 22: Model I Relationship Between RGA Score and Percentile Stream Power

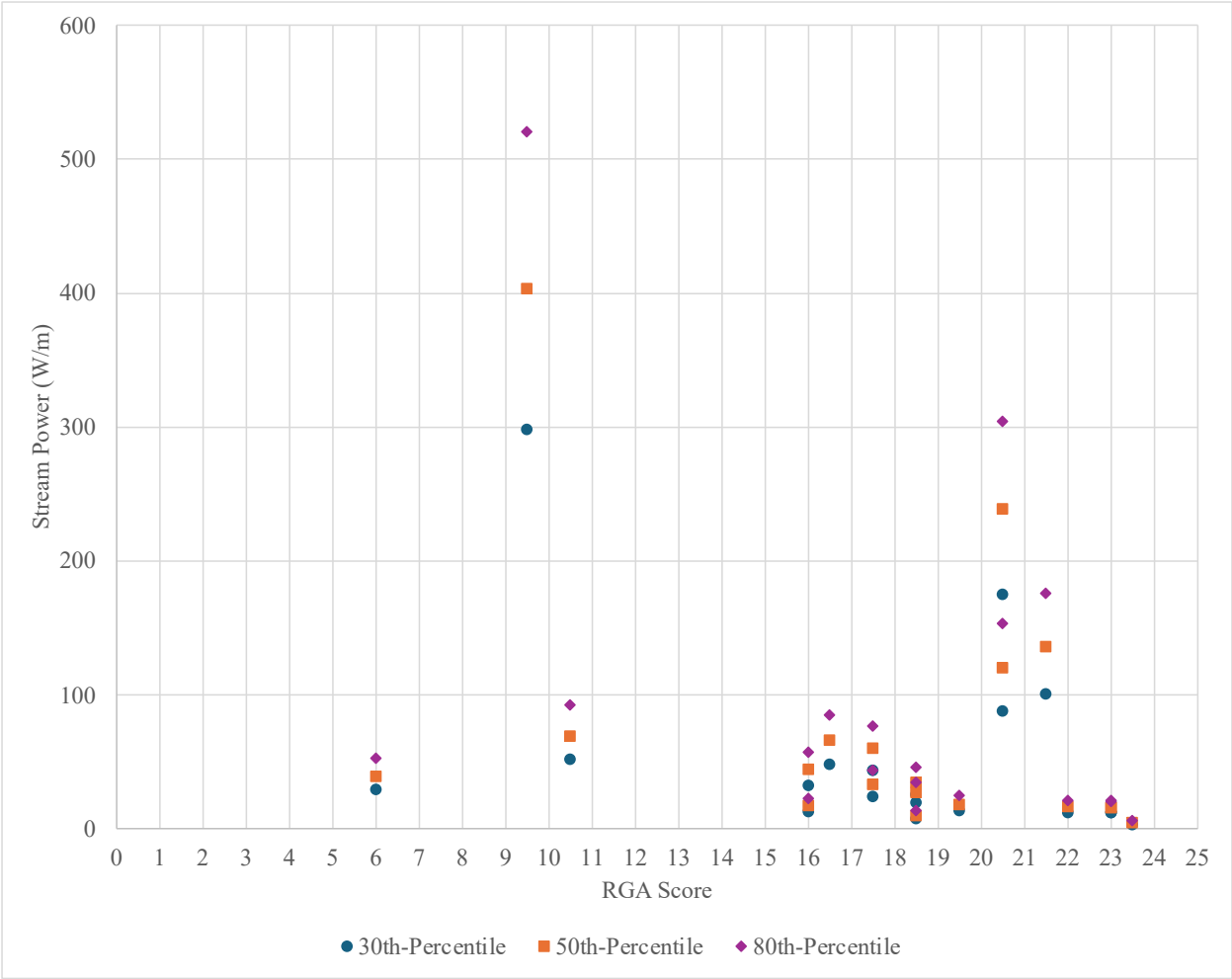


Figure 23: Model II Relationship Between RGA Score and Percentile Stream Power

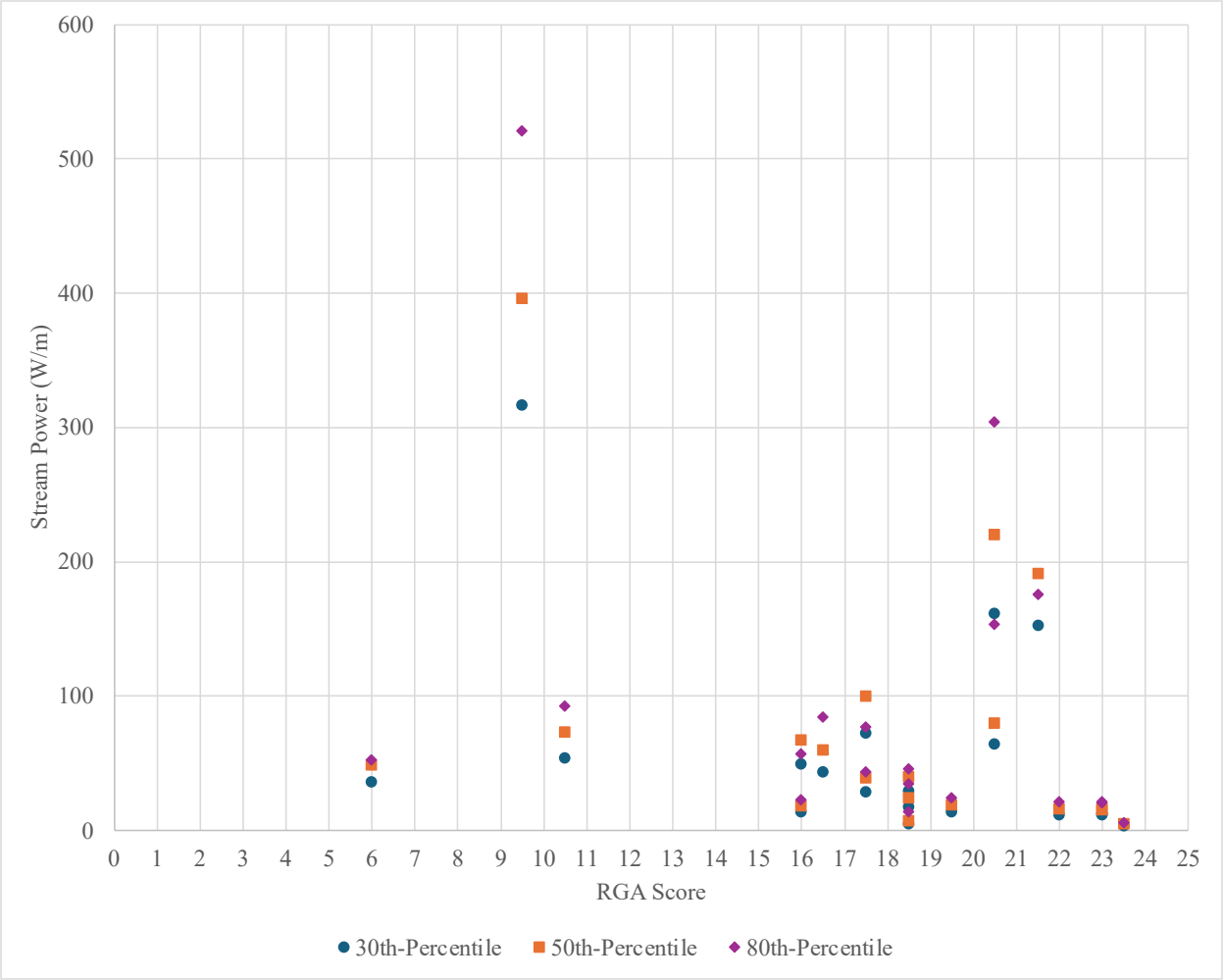


Figure 24: Model III Relationship Between RGA Score and Percentile Stream Power

Table 3: Single Regression Analysis Results

		R^2	P, F_{sig}	F
τ_{30} (Pa)	Model I	0.015	0.614	0.264
	Model II	0.166	0.083	3.382
	Model III	0.158	0.092	3.189
τ_{50} (Pa)	Model I	0.012	0.654	0.208
	Model II	0.170	0.080	3.478
	Model III	0.175	0.075	3.609
τ_{80} (Pa)	Model I	0.010	0.677	0.180
	Model II	0.182	0.069	3.770
	Model III	0.194	0.059	4.102
Ω_{30} (W/m)	Model I	0.040	0.409	0.715
	Model II	0.108	0.169	2.061
	Model III	0.115	0.156	2.208
Ω_{50} (W/m)	Model I	0.038	0.426	0.664
	Model II	0.107	0.173	2.028
	Model III	0.115	0.155	2.213
Ω_{80} (W/m)	Model I	0.036	0.438	0.631
	Model II	0.110	0.165	2.108
	Model III	0.118	0.150	2.268

Table 4: 30th-Percentile Bed Shear Stress Exclusive Stepwise Linear Multiple Regression Analysis Results

	Independent Variable	P		Independent Variable	P		Independent Variable	P
Model I τ_{30} (Pa), $R^2 = 0.348$, $F = 2.603$, $F_{sig} = 0.075$	Longest Distance Between HGCs	0.030	Model II τ_{30} (Pa), $R^2 = 0.670$, $F = 5.568$, $F_{sig} = 0.007$	Primary Bed Material	0.213	Model III τ_{30} (Pa), $R^2 = 0.739$, $F = 7.371$, $F_{sig} = 0.002$	Primary Bed Material	0.160
	Average Distance Between HGCs	0.125		Percent Forested Land Use Above Reach	0.120		Percent Forested Land Use Above Reach	0.065
	Bed/Bank Protection	0.335		Occurrence of Bank Accretion (Left Bank)	0.075		Longest Distance Between HGCs	0.030
	Degree of Incision	0.031		Stream Bank Erosion (Right Bank)	0.039		Established Riparian Woody-Vegetative Cover (Left Bank)	0.012
	Degree of Constriction	0.102		Established Riparian Woody-Vegetative Cover (Left Bank)	0.123		Degree of Incision	0.018
	Established Riparian Woody-Vegetative Cover (Left Bank)	0.139		Degree of Incision	0.086		Degree of Constriction	0.070
	---	---		Stream Bank Instability (Left Bank)	0.140		Percent Urban Land Use Above Reach	0.100
	---	---		Percent Urban Land Use Above Reach	0.164		Stage of Channel Evolution	0.294

Table 5: 50th-Percentile Bed Shear Stress Exclusive Stepwise Linear Multiple Regression Analysis Results

	Independent Variable	P		Independent Variable	P		Independent Variable	P
Model I τ_{50} (Pa), $R^2 = 0.584$, $F = 4.611$, $F_{sig} = 0.012$	Longest Distance Between HGCs	<0.001	Model II τ_{50} (Pa), $R^2 = 0.668$, $F = 5.519$, $F_{sig} = 0.007$	Primary Bed Material	0.208	Model III τ_{50} (Pa), $R^2 = 0.741$, $F = 8.370$, $F_{sig} = 0.001$	Primary Bed Material	0.145
	Average Distance Between HGCs	0.001		Percent Forested Land Use Above Reach	0.135		Percent Forested Land Use Above Reach	0.109
	Stream Bank Erosion (Right Bank)	0.003		Occurrence of Bank Accretion (Left Bank)	0.075		Established Riparian Woody-Vegetative Cover (Left Bank)	0.014
	Stream Bank Instability (Right Bank)	0.085		Stream Bank Erosion (Right Bank)	0.039		Longest Distance Between HGCs	0.019
	Occurrence of Bank Accretion (Left Bank)	0.014		Established Riparian Woody-Vegetative Cover (Left Bank)	0.121		Degree of Incision	0.025
	Bed/Bank Protection	0.004		Degree of Incision	0.082		Degree of Constriction	0.127
	Stream Bank Instability (Left Bank)	0.297		Stream Bank Instability (Left Bank)	0.147		Percent Urban Land Use Above Reach	0.177
	---	---		Percent Urban Land Use Above Reach	0.183		---	---

Table 6: 80th-Percentile Bed Shear Stress Exclusive Stepwise Linear Multiple Regression Analysis Results

	Independent Variable	P		Independent Variable	P		Independent Variable	P
Model I τ_{80} (Pa), $R^2 = 0.244$, $F = 2.450$, $F_{sig} = 0.095$	Longest Distance Between HGCs	0.011	Model II τ_{80} (Pa), $R^2 = 0.680$, $F = 5.781$, $F_{sig} = 0.006$	Primary Bed Material	0.206	Model III τ_{80} (Pa), $R^2 = 0.753$, $F = 8.819$, $F_{sig} = <0.001$	Primary Bed Material	0.151
	Average Distance Between HGCs	0.034		Percent Forested Land Use Above Reach	0.133		Percent Forested Land Use Above Reach	0.108
	Bed/Bank Protection	0.091		Occurrence of Bank Accretion (Left Bank)	0.062		Established Riparian Woody-Vegetative Cover (Left Bank)	0.010
	Degree of Incision	0.175		Stream Bank Erosion (Right Bank)	0.029		Longest Distance Between HGCs	0.015
	---	---		Established Riparian Woody-Vegetative Cover (Left Bank)	0.102		Degree of Incision	0.018
	---	---		Degree of Incision	0.072		Degree of Constriction	0.112
	---	---		Stream Bank Instability (Left Bank)	0.139		Percent Urban Land Use Above Reach	0.171
	---	---		Percent Urban Land Use Above Reach	0.175		---	---

Table 7: 30th-Percentile Stream Power Exclusive Stepwise Linear Multiple Regression Analysis Results

	Independent Variable	P		Independent Variable	P		Independent Variable	P
Model I Ω_{30} (W/m), $R^2 = 0.864$, $F = 13.665$, $F_{sig} = <0.001$	Longest Distance Between HGCs	<0.001	Model II Ω_{30} (W/m), $R^2 = 0.686$, $F = 6.612$, $F_{sig} = 0.003$	Primary Bed Material	0.108	Model III Ω_{30} (W/m), $R^2 = 0.770$, $F = 11.020$, $F_{sig} = <0.001$	Primary Bed Material	0.066
	Established Riparian Woody-Vegetative Cover (Left Bank)	<0.001		Percent Forested Land Use Above Reach	0.352		Percent Forested Land Use Above Reach	0.183
	Degree of Incision	<0.001		Longest Distance Between HGCs	0.015		Longest Distance Between HGCs	<0.001
	Degree of Constriction	0.004		Established Riparian Woody-Vegetative Cover (Left Bank)	0.004		Established Riparian Woody-Vegetative Cover (Left Bank)	<0.001
	Occurrence of Bank Accretion (Right Bank)	0.005		Degree of Incision	0.007		Degree of Incision	0.004
	Stream Bank Instability (Right Bank)	0.007		Degree of Constriction	0.025		Degree of Constriction	0.008
	Percent Forested Land Use Above Reach	0.148		Occurrence of Bank Accretion (Left Bank)	0.184		---	---
	Stage of Channel Evolution	0.022		---	---		---	---
	Primary Bed Material	0.097		---	---		---	---

Table 8: 50th-Percentile Stream Power Exclusive Stepwise Linear Multiple Regression Analysis Results

	Independent Variable	P		Independent Variable	P		Independent Variable	P
Model I Ω_{50} (W/m), $R^2 = 0.860$, F = 13.292, $F_{sig} = <0.001$	Longest Distance Between HGCs	<0.001	Model II Ω_{50} (W/m), $R^2 = 0.684$, F = 6.562, $F_{sig} = 0.003$	Primary Bed Material	0.106	Model III Ω_{50} (W/m), $R^2 = 0.743$, F = 9.669, $F_{sig} <0.001$	Primary Bed Material	0.061
	Established Riparian Woody-Vegetative Cover (Left Bank)	<0.001		Percent Forested Land Use Above Reach	0.345		Percent Forested Land Use Above Reach	0.174
	Degree of Incision	<0.001		Longest Distance Between HGCs	0.016		Longest Distance Between HGCs	<0.001
	Degree of Constriction	0.005		Established Riparian Woody-Vegetative Cover (Left Bank)	0.004		Established Riparian Woody-Vegetative Cover (Left Bank)	0.001
	Occurrence of Bank Accretion (Right Bank)	0.006		Degree of Incision	0.007		Degree of Incision	0.007
	Stream Bank Instability (Right Bank)	0.007		Degree of Constriction	0.026		Degree of Constriction	0.014
	Percent Forested Land Use Above Reach	0.181		Occurrence of Bank Accretion (Left Bank)	0.185		---	---
	Stage of Channel Evolution	0.023		---	---		---	---
	Primary Bed Material	0.089		---	---		---	---

Table 9: 80th-Percentile Stream Power Exclusive Stepwise Linear Multiple Regression Analysis Results

	Independent Variable	P		Independent Variable	P		Independent Variable	P
Model I Ω_{80} (W/m), $R^2 = 0.858$, $F = 13.038$, $F_{sig} = <0.001$	Longest Distance Between HGCs	<0.001	Model II Ω_{80} (W/m), $R^2 = 0.687$, $F = 6.648$, $F_{sig} = 0.003$	Primary Bed Material	0.105	Model III Ω_{80} (W/m), $R^2 = 0.735$, $F = 9.302$, $F_{sig} = <0.001$	Primary Bed Material	0.059
	Established Riparian Woody-Vegetative Cover (Left Bank)	0.001		Percent Forested Land Use Above Reach	0.356		Percent Forested Land Use Above Reach	0.172
	Degree of Incision	<0.001		Longest Distance Between HGCs	0.015		Longest Distance Between HGCs	0.001
	Degree of Constriction	0.005		Established Riparian Woody-Vegetative Cover (Left Bank)	0.004		Established Riparian Woody-Vegetative Cover (Left Bank)	0.002
	Occurrence of Bank Accretion (Right Bank)	0.006		Degree of Incision	0.007		Degree of Incision	0.008
	Stream Bank Instability (Right Bank)	0.008		Degree of Constriction	0.024		Degree of Constriction	0.016
	Percent Forested Land Use Above Reach	0.211		Occurrence of Bank Accretion (Left Bank)	0.183		---	---
	Stage of Channel Evolution	0.023		---	---		---	---
	Primary Bed Material	0.085		---	---		---	---

Table 10: 30th-Percentile Bed Shear Stress Inclusive Stepwise Linear Multiple Regression Analysis Results

	Independent Variable	P		Independent Variable	P		Independent Variable	P
Model I τ_{30} (Pa), $R^2 = 0.925$, F = 38.164, F_{sig} = <0.001	S_{avg}	<0.001	Model II τ_{30} (Pa), $R^2 = 0.905$, F = 44.027, F_{sig} = <0.001	Drainage Area	<0.001	Model III τ_{30} (Pa), $R^2 = 0.969$, F = 70.843, F_{sig} = <0.001	Drainage Area	<0.001
	Occurrence of Bank Accretion (Left Bank)	0.009		S_{avg}	<0.001		S_{avg}	<0.001
	Stream Bank Erosion (Left Bank)	0.006		Percent Urban Land Use Above Reach	0.140		Stream Bank Erosion (Right Bank)	0.080
	Stage of Channel Evolution	0.021		Degree of Constriction	0.186		Stream Bank Erosion (Left Bank)	0.048
	Longest Distance Between HGCs	0.051		---	---		Percent Forested Land Use Above Reach	0.099
	Percent Urban Land Use Above Reach	0.006		---	---		Degree of Incision	0.069
	---	---		---	---		Longest Distance Between HGCs	0.161
	---	---		---	---		Stream Bank Instability (Left Bank)	0.253

Table 11: 50th-Percentile Bed Shear Stress Inclusive Stepwise Linear Multiple Regression Analysis Results

	Independent Variable	P		Independent Variable	P		Independent Variable	P
Model I τ_{50} (Pa), $R^2 = 0.933$, $F = 36.876$, $F_{sig} = <0.001$	S_{avg}	<0.001	Model II τ_{50} (Pa), $R^2 = 0.901$, $F = 42.051$, $F_{sig} = <0.001$	S_{avg}	<0.001	Model III τ_{50} (Pa), $R^2 = 0.961$, $F = 110.594$, $F_{sig} = <0.001$	Drainage Area	<0.001
	Occurrence of Bank Accretion (Left Bank)	0.013		Drainage Area	<0.001		S_{avg}	<0.001
	Stream Bank Erosion (Left Bank)	0.005		Percent Urban Land Use Above Reach	0.129		Stream Bank Erosion (Right Bank)	0.113
	Stage of Channel Evolution	0.027		Degree of Constriction	0.184		Degree of Constriction	0.208
	Percent Forested Land Use Above Reach	0.008		---	---		---	---
	Longest Distance Between HGCs	0.049		---	---		---	---
	Drainage Area	0.222		---	---		---	---

Table 12: 80th-Percentile Bed Shear Stress Inclusive Stepwise Linear Multiple Regression Analysis Results

	Independent Variable	P		Independent Variable	P		Independent Variable	P
Model I τ_{80} (Pa), $R^2 = 0.941$, $F = 42.163$, $F_{sig} = <0.001$	S_{avg}	<0.001	Model II τ_{80} (Pa), $R^2 = 0.911$, $F = 47.156$, $F_{sig} = <0.001$	S_{avg}	<0.001	Model III τ_{80} (Pa), $R^2 = 0.963$, $F = 94.250$, $F_{sig} = <0.001$	Drainage Area	<0.001
	Occurrence of Bank Accretion (Left Bank)	0.012		Drainage Area	<0.001		S_{avg}	<0.001
	Stream Bank Erosion (Left Bank)	0.004		Percent Urban Land Use Above Reach	0.149		Degree of Constriction	0.175
	Stage of Channel Evolution	0.028		Degree of Constriction	0.182		Stream Bank Erosion (Left Bank)	0.149
	Percent Forested Land Use Above Reach	0.010		---	---		Established Riparian Woody-Vegetative Cover (Right Bank)	0.216
	Longest Distance Between HGCs	0.037		---	---		---	---
	Drainage Area	0.199		---	---		---	---

Table 13: 30th-Percentile Stream Power Inclusive Stepwise Linear Multiple Regression Analysis Results

	Independent Variable	P		Independent Variable	P		Independent Variable	P
Model I Ω_{30} (W/m), R^2 = 0.945, F = 39.384, F_{sig} = <0.001	S_{avg}	<0.001	Model II Ω_{30} (W/m), R^2 = 0.960, F = 54.561, F_{sig} = <0.001	Drainage Area	<0.001	Model III Ω_{30} (W/m), R^2 = 0.958, F = 51.813, F_{sig} = <0.001	Drainage Area	<0.001
	Drainage Area	0.009		S_{avg}	<0.001		S_{avg}	<0.001
	Longest Distance Between HGCs	<0.001		Bed/Bank Protection	<0.001		Bed/Bank Protection	<0.001
	Occurrence of Bank Accretion (Left Bank)	<0.001		Established Riparian Woody-Vegetative Cover (Left Bank)	0.002		Established Riparian Woody-Vegetative Cover (Left Bank)	0.019
	Stream Bank Erosion (Left Bank)	<0.001		Stream Bank Erosion (Right Bank)	0.048		Shortest Distance Between HGCs	0.074
	Stage of Channel Evolution	0.002		Shortest Distance Between HGCs	0.010		Average Distance Between HGCs	0.165
	Percent Urban Land Use Above Reach	0.022		Longest Distance Between HGCs	0.026		Stream Bank Instability (Right Bank)	0.246
	Degree of Incision	0.253		Degree of Constriction	0.170		Established Riparian Woody-Vegetative Cover (Right Bank)	0.294

Table 14: 50th-Percentile Stream Power Inclusive Stepwise Linear Multiple Regression Analysis Results

	Independent Variable	P		Independent Variable	P		Independent Variable	P
Model I Ω_{50} (W/m), $R^2 = 0.946$, $F = 40.177$, $F_{sig} = <0.001$	S_{avg}	<0.001	Model II Ω_{50} (W/m), $R^2 = 0.960$, $F = 54.586$, $F_{sig} = <0.001$	Drainage Area	<0.001	Model III Ω_{50} (W/m), $R^2 = 0.962$, $F = 57.392$, $F_{sig} = <0.001$	Drainage Area	<0.001
	Drainage Area	0.011		S_{avg}	<0.001		S_{avg}	<0.001
	Longest Distance Between HGCs	<0.001		Bed/Bank Protection	<0.001		Bed/Bank Protection	<0.001
	Occurrence of Bank Accretion (Left Bank)	<0.001		Established Riparian Woody-Vegetative Cover (Left Bank)	0.002		Established Riparian Woody-Vegetative Cover (Left Bank)	0.017
	Stream Bank Erosion (Left Bank)	<0.001		Stream Bank Erosion (Right Bank)	0.051		Shortest Distance Between HGCs	0.027
	Stage of Channel Evolution	0.002		Shortest Distance Between HGCs	0.009		Average Distance Between HGCs	0.062
	Percent Urban Land Use Above Reach	0.024		Longest Distance Between HGCs	0.023		Established Riparian Woody-Vegetative Cover (Right Bank)	0.168
	Degree of Incision	0.238		Degree of Constriction	0.161		Stream Bank Instability (Left Bank)	0.245

Table 15: 80th-Percentile Stream Power Inclusive Stepwise Linear Multiple Regression Analysis Results

	Independent Variable	P		Independent Variable	P		Independent Variable	P
Model I Ω_{80} (W/m), $R^2 = 0.946$, $F = 40.517$, $F_{sig} = <0.001$	S_{avg}	<0.001	Model II Ω_{80} (W/m), $R^2 = 0.960$, $F = 54.541$, $F_{sig} = <0.001$	Drainage Area	<0.001	Model III Ω_{80} (W/m), $R^2 = 0.962$, $F = 58.300$, $F_{sig} = <0.001$	Drainage Area	<0.001
	Drainage Area	0.012		S_{avg}	<0.001		S_{avg}	<0.001
	Longest Distance Between HGCs	<0.001		Bed/Bank Protection	<0.001		Bed/Bank Protection	<0.001
	Occurrence of Bank Accretion (Left Bank)	<0.001		Established Riparian Woody-Vegetative Cover (Left Bank)	0.002		Established Riparian Woody-Vegetative Cover (Left Bank)	0.016
	Stream Bank Erosion (Left Bank)	<0.001		Stream Bank Erosion (Right Bank)	0.050		Shortest Distance Between HGCs	0.022
	Stage of Channel Evolution	0.002		Shortest Distance Between HGCs	0.011		Average Distance Between HGCs	0.048
	Percent Urban Land Use Above Reach	0.028		Longest Distance Between HGCs	0.028		Established Riparian Woody-Vegetative Cover (Right Bank)	0.157
	Degree of Incision	0.224		Degree of Constriction	0.174		Stream Bank Instability (Left Bank)	0.238

For $\tau_{30,50,80}$, R^2 values ranged from 0.244 to 0.753 in exclusive models and 0.901 to 0.969 in inclusive models. Additionally, F values ranged from 2.450 to 8.819 in exclusive models and 36.876 to 110.594 in inclusive models. F_{sig} values ranged from <0.001 to 0.095 in exclusive models and equaled <0.001 in inclusive models. R^2 and F values increased and F_{sig} values decreased in exclusive $\tau_{30,50,80}$ models from Model I to Model III. In inclusive models, F values increased from Model I to Model III, while Models II and III yielded the smallest and largest R^2 values, respectively. Despite the performance of Model II, all R^2 values in $\tau_{30,50,80}$ inclusive models were greater than 0.9 suggesting consistency among models. The slightly worse performance of Model II was likely because the smallest group of independent variables was included in each percentile analysis. From comparing percentiles of exclusive models, Model III R^2 and F values increased and F_{sig} decreased with increasing percentile, and Model I and Model II yielded relatively consistent results. Inclusive percentile models yielded consistent R^2 and F values. Analysis reach slope (S_{avg}) and drainage area dominated inclusive models as highly significant independent variables. Primary bed material, degree of incision, degree of constriction, established riparian woody-vegetative cover (left bank), percent urban land use above reach, percent forested land use above reach, and longest distance between HGCs were frequently included variables in $\tau_{30,50,80}$ exclusive models.

For $\Omega_{30,50,80}$, R^2 values ranged from 0.684 to 0.864 in exclusive models and 0.945 to 0.962 in inclusive models. Additionally, F values ranged from 6.562 to 13.665 in exclusive models and 39.384 to 58.300 in inclusive models. F_{sig} values ranged from <0.001 to 0.003 in exclusive models and equaled <0.001 in inclusive models. In exclusive models, R^2 and F values were largest and F_{sig} values were smallest in Model I followed by Model III. The outperformance of Model I compared to Models II and III was likely caused by the inclusion of more independent variables and the order in which independent variables were included. R^2 and F values in inclusive models were consistent between Models II and III and smaller in Model I. From comparing percentiles of exclusive models, Models I and III R^2 and F values slightly decreased and F_{sig} slightly increased with increasing percentile, and Model II yielded relatively consistent results. Similarly to $\tau_{30,50,80}$ analyses, inclusive percentile models yielded consistent R^2 and F values. S_{avg} and drainage area

dominated inclusive models. Except for percent urban land use above reach, the same frequently included variables that predicted $\tau_{30,50,80}$ were also included in $\Omega_{30,50,80}$ exclusive models.

CHAPTER FOUR
DISCUSSION

The study objectives were to determine the level of model development necessary to plan and prioritize watershed enhancement activities, SCM implementation and/or stream restoration, and to explore the correlation among field reconnaissance data, desktop-gathered data, and modeled stream power and bed shear stress for a portion of the Turkey Creek watershed in Knox County, Tennessee. The respective effectiveness of geomorphic node placement and inclusion of SCMs into watershed-scale models were assessed within the scope of the study. Model III outperformed other model simulations indicating that watershed planning models should incorporate geomorphic node placement, stormwater control measures (SCMs), desktop data, field verification, and manual adjustment of features automatically generated by model software. Additionally, field reconnaissance and desktop-gathered data correlated to percentile stream power ($\Omega_{30,50,80}$) and bed shear stress ($\tau_{30,50,80}$). Interestingly, some rapid geomorphic assessment (RGA) metrics correlated to $\Omega_{30,50,80}$ and $\tau_{30,50,80}$, while others showed little correlation. Also, longest distance between hydraulic grade controls (HGCs) was included as a statistically significant independent variable in multiple regression models highlighting the importance of geomorphic node placement in watershed planning models. For single and stepwise linear multiple regression analyses, little variation of coefficient of determination (R^2) values was found among percentile regression models. Ultimately, this study points towards a geomorphic-based modeling approach for urban watershed planning and shows that building a living watershed-scale model provides a stormwater manager the key information to locate areas of instability and test rehabilitation techniques to offset urban hydromodification.

Suggested Level of Model Development for Watershed Management Planning

Based on the results, Model III outperformed other model development simulations indicating that models generated for watershed planning should incorporate geomorphic node placement, stormwater control measures (SCMs), desktop data, field verification, and manual adjustment of features automatically generated by model software. Although Model I maximum stream power

(Ω_{max}) and bed shear stress (τ_{max}) averages were considered invalid due to adverse model slopes, the decrease in averages from Model II to Model III suggested that modeling SCMs provided flow attenuation. Ω_{max} and τ_{max} averages decreased from Model II to Model III by 18.9 pascals and 1,053.0 watts per meter, respectively. While it is likely SCMs provided attenuation, the additional channel conduits included in Model III may have skewed averages, as the added conduits visually appeared in lower Ω_{max} and τ_{max} ranges in Figures 15 and 18. Additionally, wide ranges of Ω_{max} and τ_{max} for each model simulation were products of conduit discharge and slope variation, as conduits represented channel segments throughout the study watershed ranging from headwater conveyances and SCM outlets to main channel stems. Regardless of Ω_{max} and τ_{max} findings, Model III yielded the highest R^2 values during all single regression analyses except for the analysis of 30^{th}-percentile bed shear stress (τ_{30}). All resulting R^2 values from single regression analyses were below the minimum value of 0.7 for this study, but Model III R^2 values were consistently higher compared to the other model simulations. Additionally, Model I R^2 values were an order of magnitude lower than that of the other model simulations, suggesting that Model I did not correlate with RGA scores whatsoever.

Stepwise linear multiple regression analyses further supported Model III as the best example model for watershed planning, since exclusive regression model R^2 values were all greater than the minimum threshold of 0.7. Model III outperformed Model II in all exclusive multiple regression models, but Model I actually outperformed Model III in exclusive stream power models. Despite the high average Model I R^2 value of 0.861, Model III was considered to be more accurate, since Model I performed poorly in single regression analyses and included adverse conduit slopes. As for inclusive multiple regression models, all model simulations performed exceptionally well as drainage area and analysis reach slope (S_{avg}) were consistently included as highly significant independent variables and likely skewed model results. Compared to Model II and Model III, Model I inclusive multiple regression models either did not include drainage area as a significant variable or included drainage area with a relatively high significance (P) value, suggesting that automatically generated subcatchment boundaries in PCSWMM did not accurately represent true drainage areas.

Correlation Among Field Reconnaissance Data, Desktop-Gathered Data, and Percentile Stream Power and Bed Shear Stress

Single and stepwise linear multiple regression analyses yielded varying results, but field reconnaissance data and desktop-gathered data were determined to be significant predictors of $\Omega_{30,50,80}$ and $\tau_{30,50,80}$. As previously discussed, all single regression analysis R^2 values were less than 0.7, suggesting that RGA score did not relate to $\Omega_{30,50,80}$ and $\tau_{30,50,80}$. Conversely, exclusive multiple regression analyses included RGA sub-metrics as significant independent variables. For the purpose of this discussion, inclusive multiple regression models were ignored, since drainage area and S_{avg} likely skewed results. $\tau_{30,50,80}$ exclusive regression models frequently included primary bed material, degree of incision, degree of constriction, established riparian woody-vegetative cover (left bank), percent urban land use above reach, percent forested land use above reach, and longest distance between HGCs as significant independent variables. $\Omega_{30,50,80}$ exclusive regression models included the same variables except for percent urban land use above reach. These variables represent a combination of field reconnaissance and desktop-gathered data and highlight the importance of geomorphic node placement, since the longest distance between HGCs was included in most exclusive regression models as an indicator of vertical instability. Additionally, the inclusion of percent forested land use above reach aligns with previous study results suggesting that stream bank vegetation and forestation help to maintain ecological and geomorphological function in both rural and urban watersheds (Hession et al., 2003; Sweeney et al., 2004).

Benefits of Geomorphic-Based Modeling Approach for Urban Watershed Planning

A geomorphic-based modeling approach for urban watershed planning has potential to expand and improve upon previous watershed planning ideologies by offering a method of identifying and prioritizing areas of channel instability based on effective impervious area (EIA), HGC locations, and RGAs, maintaining a database of stream, SCM, and stormwater infrastructure survey and design data, testing rehabilitation projects prior to construction, and predicting effects of new development. Earles et al., (2020) and Vietz et al., (2014) utilized geomorphic field assessments

for project selection and correlation analysis between geomorphology and EIA, respectively. Additionally, Vietz et al., (2014) showed that measurable geomorphic changes occur even at low levels of EIA (0-3%) which supports the claim by Walsh, Fletcher, & Ladson, (2005) that EIA is the dominant cause of stream degradation in urban watersheds. Although total impervious area (TIA) was used to model the study watershed (due to limited data availability), PCSWMM is capable of modeling EIA if the user builds detailed subcatchments that reflect stormwater infrastructure and impervious surfaces and/or models subcatchments using impervious subcatchment routing. In PCSWMM, impervious subcatchment routing directs rainfall onto impervious surfaces before reaching a subcatchment's outlet node.

To properly model watershed conditions and EIA, adequate stream, SCM, and stormwater infrastructure data is necessary when building more detailed subcatchments compared to those modeled in this study. The need for a living database could encourage stormwater managers to house data using a software like ArcGIS Pro, so data could be easily accessed and viewed spatially. As presented in this study, analysis reaches within an urban watershed can be defined by HGC locations, land use changes, RGAs, and channel confluences, and EIA can be used to model bed shear stress and stream power in order to identify and prioritize rehabilitation projects. Although some RGA metrics were not included as statistically significant independent variables in exclusive multiple regression models, metrics such as primary bed material, degree of incision, degree of constriction, established riparian woody-vegetative cover (left bank) along with other data such as percent urban land use above reach (only included for $\tau_{30,50,80}$ models), percent forested land use above reach, and longest distance between HGCs correlated to bed shear stress and stream power highlighting the need to incorporate geomorphic data into a modeling approach for urban watershed planning.

A key benefit of a geomorphic-based modeling approach for urban watershed planning is the ability to test the effectiveness of potential rehabilitation projects prior to construction. Without modeling, watershed planning frameworks incorporating master planning, design, and construction must rely on a case-by-case basis of project success post-construction to guide prioritization of future projects (Earles et al., 2020). Additionally, Walsh, Fletcher, & Ladson, (2005), Earles et al., (2020), and Vietz et al., (2014) have argued that successful stream restoration

requires SCMs or other methods of increasing infiltration or bioretention to be implemented to reduce geomorphologically effective stream flows. With a model, the effectiveness of paired SCM and stream restoration projects may be assessed along with the potential effect of new development upstream or adjacent to the project area. New development can undermine restoration projects as a result of increased impervious area draining to streams (Prosser, Morison, & Coleman, 2015; Walsh et al., 2016; Walsh et al., 2015). Although prioritizing and modeling the effectiveness of projects was beyond the scope of this study, the study methodology provides a foundation to build a watershed assessment framework incorporating geomorphic-based hydrologic and hydraulic modeling.

Conclusions and Recommendations

To create an urban watershed assessment framework involving the planning and prioritization of enhancement practices such as stream restoration and SCM implementation, a geomorphologically-relevant watershed-scale model must be built to assess existing and potential watershed function. Ideally, stormwater managers would utilize a watershed-scale model as a living tool to test the performance of potential rehabilitation activities rather than determining project success on a case-by-case basis post-construction. From this study, Model III was found to be the most appropriate model for watershed planning, since its level of model development incorporated geomorphic node placement, SCMs, desktop data, field verification, and manual adjustment of features automatically generated by model software. Model II, which excluded SCMs during model development, only performed slightly worse compared to Model III. Therefore, Model II could be substituted as an example watershed-scale model when no SCM data is available. In this study, Model III would have likely performed better and represented more attenuation if SCM data had been available. In terms of proper model development, the best-case scenario would be for a stormwater manager to have access to stream survey and SCM data across the watershed. From there, stormwater managers could maintain the model as either new development or rehabilitation practices occur within the watershed.

In terms of data correlation, field-reconnaissance and desktop-gathered data generally corresponded to $\Omega_{30,50,80}$ and $\tau_{30,50,80}$. Although RGA scores were not significantly related to

$\Omega_{30,50,80}$ and $\tau_{30,50,80}$, some RGA sub-metrics were included in most exclusive stepwise linear multiple regression models. Land uses and longest distance to HGCs were also frequently included, suggesting that a combination of field and desktop data should be incorporated during watershed-scale model development. Building a living watershed-scale planning model with geomorphic relevance provides a stormwater manager the key information to locate areas of instability and test rehabilitation techniques to offset urban hydromodification.

LIST OF REFERENCES

Anim, D. O., Fletcher, T. D., Pasternack, G. B., Vietz, G. J., Duncan, H. P., & Burns, M. J. (2019). Can catchment-scale urban stormwater management measures benefit the stream hydraulic environment? *Journal of environmental management*, *233*, 1-11. https://doi.org/10.1016/j.jenvman.2018.12.023

Bernhardt, E. S., & Palmer, M. A. (2011). River restoration: the fuzzy logic of repairing reaches to reverse catchment scale degradation. *Ecological applications*, *21*(6), 1926-1931. https://doi.org/10.1890/10-1574.1

Bizzi, S., & Lerner, D. N. (2015). The Use of Stream Power as an Indicator of Channel Sensitivity to Erosion and Deposition Processes. *River research and applications*, *31*(1), 16-27. https://doi.org/10.1002/rra.2717

Bledsoe, B. P., Stein, E. D., Hawley, R. J., & Booth, D. (2012). Framework and Tool for Rapid Assessment of Stream Susceptibility to Hydromodification. *Journal of the American Water Resources Association*, *48*(4), 788-808. https://doi.org/10.1111/j.1752-1688.2012.00653.x

Booth, D. B., & Fischenich, C. J. (2015). A channel evolution model to guide sustainable urban stream restoration: An urban channel evolution model. *Area (London 1969)*, *47*(4), 408-421. https://doi.org/10.1111/area.12180

Brunner, G. W. (2021). HEC-RAS 2D User's Manual Version 6.5. In. Hydrologic Engineering Center: US Army Corps of Engineers.

Buchanan, T. J., & Somers, W. P. (1969). *Discharge measurements at gaging stations* [Report](03-A8). (Techniques of Water-Resources Investigations, Issue. U. S. G. P. Office. https://pubs.usgs.gov/publication/twri03A8

Burns, M. J., Fletcher, T. D., Walsh, C. J., Ladson, A. R., & Hatt, B. E. (2012). Hydrologic shortcomings of conventional urban stormwater management and opportunities for reform. *Landscape and Urban Planning*, *105*(3), 230-240. https://doi.org/https://doi.org/10.1016/j.landurbplan.2011.12.012

Cousins, J. J., & Hill, D. T. (2021). Green infrastructure, stormwater, and the financialization of municipal environmental governance. *Journal of Environmental Policy & Planning*, *23*(5), 581-598. https://doi.org/10.1080/1523908X.2021.1893164

dos Reis Oliveira, P. C., van der Geest, H. G., Kraak, M. H. S., Westveer, J. J., Verdonschot, R. C. M., & Verdonschot, P. F. M. (2020). Over forty years of lowland stream restoration: Lessons learned? *Journal of environmental management*, *264*, 110417-110417. https://doi.org/10.1016/j.jenvman.2020.110417

Earles, A., Chongtoua, B., Clary, J., & Zivkovich, B. (2020). Estimation of Pollutant Load Reductions from Restoration of Cherry Creek in Denver. *Journal of sustainable water in the built environment*, *6*(3). https://doi.org/10.1061/JSWBAY.0000918

Epps, T. H., & Hathaway, J. M. (2018). Establishing a Framework for the Spatial Identification of Effective Impervious Areas in Gauged Basins: Review and Case Study. *Journal of sustainable water in the built environment*, *4*(2). https://doi.org/10.1061/JSWBAY.0000853

Hawley, R. J., Russell, K., & Taniguchi-Quan, K. (2022). Restoring geomorphic integrity in urban streams via mechanistically-based storm water management: minimizing excess sediment transport capacity. *Urban Ecosystems*, *25*(4), 1247-1264. https://doi.org/10.1007/s11252-022-01221-y

Hession, W. C., Pizzuto, J. E., Johnson, T. E., & Horwitz, R. J. (2003). Influence of bank vegetation on channel morphology in rural and urban watersheds. *Geology*, *31*(2), 147-150. https://doi.org/10.1130/0091-7613(2003)031<0147:IOBVOC>2.0.CO;2

Lea, D. M., & Legleiter, C. J. (2016). Mapping spatial patterns of stream power and channel change along a gravel-bed river in northern Yellowstone. *Geomorphology (Amsterdam, Netherlands)*, *252*, 66-79. https://doi.org/10.1016/j.geomorph.2015.05.033

Li, M.-H. (2008). Stream Restoration Design Handbook (National Engineering Handbook, 210-VI, Part 654), J.M. Bernard, J. Fripp, K. Robinson (Eds.), US Department of Agriculture, Natural Resources Conservation Service, 2007. In (Vol. 87, pp. 97-98): Elsevier B.V.

McCleary, R. B. (1999). A Stormwater Banking Alternative for Highway Projects. In *Proc. National Conf. on Retrofit Opport. for Water Rec Protect. in Urban Environ.* U.S. Environmental Protection Agency, Washington, DC: EPA/625/C-99/001.

Murphy, B. M., Russell, K. L., Stillwell, C. C., Hawley, R., Scoggins, M., Hopkins, K. G., Burns, M. J., Taniguchi-Quan, K. T., Macneale, K. H., & Smith, R. F. (2022). Closing the gap on wicked urban stream restoration problems: A framework to integrate science and community values. *Freshwater science*, *41*(3), 521-531. https://doi.org/10.1086/721134

Niazi, M., Nietch, C., Maghrebi, M., Jackson, N., Bennett, B. R., Tryby, M., & Massoudieh, A. (2017). Storm Water Management Model: Performance Review and Gap Analysis. *Journal of sustainable water in the built environment*, *3*(2). https://doi.org/10.1061/JSWBAY.0000817

Prosser, T., Morison, P. J., & Coleman, R. A. (2015). Integrating stormwater management to restore a stream: perspectives from a waterway management authority. *Freshwater science*, *34*(3), 1186-1194. https://doi.org/10.1086/682566

Rieck, L., Carson, C., Hawley, R. J., Heller, M., Paul, M., Scoggins, M., Zimmerman, M., & Smith, R. F. (2022). Phase II MS4 challenges: moving toward effective stormwater management for small municipalities. *Urban Ecosystems*, *25*(3), 657-672. https://doi.org/10.1007/s11252-021-01179-3

Rodak, C. M., Jayakaran, A. D., Moore, T. L., David, R., Rhodes, E. R., & Vogel, J. R. (2020). Urban stormwater characterization, control, and treatment. *Water Environment Research*, *92*(10), 1552-1586. https://doi.org/10.1002/wer.1403

Rossman, L. (2017). Storm Water Management Model Reference Manual Volume II - Hydraulics. In. U.S. Environmental Protection Agency, Washington, DC: EPA/600/R-17/111.

Rossman, L., & Huber, W. (2015). Storm Water Management Model Reference Manual Volume I, Hydrology. In. U.S. EPA Office of Research and Development, Washington, DC: EPA/600/R-15/162A.

Rossman, L., & Simon, M. (2022). Storm Water Management Model User's Manual Version 5.2. In. U.S. Environmental Protection Agency, Washington, DC: EPA/600/R-22/030.

Rubin, Z., Kondolf, G., & Rios-Touma, B. (2017). Evaluating Stream Restoration Projects: What Do We Learn from Monitoring? *Water*, *9*(3), 174. https://doi.org/10.3390/w9030174

Shields, F. D., Copeland, R. R., Klingeman, P. C., Doyle, M. W., & Simon, A. (2003). Design for Stream Restoration. *Journal of hydraulic engineering (New York, N.Y.)*, *129*(8), 575-584. https://doi.org/10.1061/(ASCE)0733-9429(2003)129:8(575)

Simon, A., & Darby, S. (1999). The nature and significance of incised river channels. In (pp. 3-18): John Wiley and Sons Ltd., Chichester, England.

Simon, A., & Downs, P. W. (1995). An interdisciplinary approach to evaluation of potential instability in alluvial channels. *Geomorphology*, *12*(3), 215-232. https://doi.org/https://doi.org/10.1016/0169-555X(95)00005-P

Simon, A., & Klimetz, L. (2008). Magnitude, Frequency, and Duration Relations for Suspended Sediment in Stable ("Reference") Southeastern Streams1. *JAWRA Journal of the American Water Resources Association*, *44*, 1270-1283. https://doi.org/10.1111/j.1752-1688.2008.00222.x

Sweeney, B. W., Bott, T. L., Jackson, J. K., Kaplan, L. A., Newbold, J. D., Standley, L. J., Hession, W. C., & Horwitz, R. J. (2004). Riparian deforestation, stream narrowing, and loss of stream ecosystem services. *Proceedings of the National Academy of Sciences*, *101*(39), 14132-14137. https://doi.org/10.1073/pnas.0405895101

Tschantz, B., Gangaware, T., & Morton, R. (2003). Tennessee Guide to the Selection and Design of Stormwater Best Management Practices (BMPs). In: Tennessee Department of Environment and Conservation Division of Water Pollution Control.

Vietz, G. J., Sammonds, M. J., Walsh, C. J., Fletcher, T. D., Rutherfurd, I. D., & Stewardson, M. J. (2014). Ecologically relevant geomorphic attributes of streams are impaired by even low levels of watershed effective imperviousness. *Geomorphology*, *206*, 67-78. https://doi.org/https://doi.org/10.1016/j.geomorph.2013.09.019

Vocal Ferencevic, M., & Ashmore, P. (2012). Creating and evaluating digital elevation model-based stream-power map as a stream assessment tool. *River research and applications*, *28*(9), 1394-1416. https://doi.org/10.1002/rra.1523

Walsh, C. J., Booth, D. B., Burns, M. J., Fletcher, T. D., Hale, R. L., Hoang, L. N., Livingston, G., Rippy, M. A., Roy, A. H., Scoggins, M., & Wallace, A. (2016). Principles for urban stormwater management to protect stream ecosystems. *Freshwater science*, *35*(1), 398-411. https://doi.org/10.1086/685284

Walsh, C. J., Fletcher, T. D., Bos, D. G., & Imberger, S. J. (2015). Restoring a stream through retention of urban stormwater runoff: a catchment-scale experiment in a social–ecological system. *Freshwater science*, *34*(3), 1161-1168. https://doi.org/10.1086/682422

Walsh, C. J., Fletcher, T. D., & Ladson, A. R. (2005). Stream restoration in urban catchments through redesigning stormwater systems: looking to the catchment to save the stream. *Journal of the North American Benthological Society*, *24*(3), 690-705. https://doi.org/10.1899/04-020.1

Walsh, C. J., Roy, A. H., Feminella, J. W., Cottingham, P. D., Groffman, P. M., & Morgan, R. P. (2005). The urban stream syndrome: current knowledge and the search for a cure. *Journal of the North American Benthological Society*, *24*(3), 706-723. https://doi.org/10.1899/04-028.1

Woockman, R. R., & Schwartz, J. S. (2018). *Rethinking channel protection efforts : an integration of fluvial geomorphology, engineering, and economics* The University of Tennessee, Knoxville]. Knoxville, Tennessee.

Wu, J., Wu, X., & Zhang, J. (2019). Development Trend and Frontier of Stormwater Management (1980–2019): A Bibliometric Overview Based on CiteSpace. *Water*, *11*(9), 1908. https://www.mdpi.com/2073-4441/11/9/1908

Zhao, J. Z., Fonseca, C., & Zeerak, R. (2019). Stormwater Utility Fees and Credits: A Funding Strategy for Sustainability. *Sustainability*, *11*(7), 1913. https://www.mdpi.com/2071-1050/11/7/1913

VITA

Matthew Joseph Tolson grew up in Knoxville, Tennessee. After graduating from Clinton High School, he attended the University of Tennessee, Knoxville and received a Bachelor of Science degree in Civil and Environmental Engineering with a minor in Watershed Studies and Applied Music for Voice. He then chose to pursue a Master of Science degree in Environmental Engineering with a concentration in Water Resources Engineering. After graduation, he will continue his career as an Environmental Designer at a local engineering firm.